Unraveling the complex nature of FS CMa stars

Nela Dvořáková

Seminář, Ondřejov

15.2.2024

B[e] phenomenon - discovery

first observed with emission line stars - Fleming (1898) - prototype **FS CMa** (HD 45677)

Strong Hα emission

Merril (1925, 1928) - identified **iron** emission lines

1928 - Hβ and Hγ - double peaked

explained by a **rotating disk**

B[e] phenomenon - discovery

first observed with emission line stars - Fleming (1898) - prototype **FS CMa** (HD 45677)

Strong Hα emission

Merril (1925, 1928) - identified **iron** emission lines

1928 - Hβ and Hγ - double peaked

explained by a **rotating disk**

Later in 1970s - IR observations

discovery of the **IR excess**

Allen & Swings (1976) - survey of ≅700 B type stars -> ≅ 65 - **IR excess as well as forbidden lines**

B[e] phenomenon - discovery

first observed with emission line stars - Fleming (1898) - prototype **FS CMa** (HD 45677)

Strong Hα emission

Merril (1925, 1928) - identified **iron** emission lines

1928 - Hβ and Hγ - double peaked

explained by a **rotating disk**

Later in 1970s - IR observations

discovery of the **IR excess**

Allen & Swings (1976) - survey of ≅700 B type stars -> ≅ 65 - **IR excess as well as forbidden lines**

=> stars with the **B[e] phenomenon**

B[e] phenomenon

Strong Balmer emissions

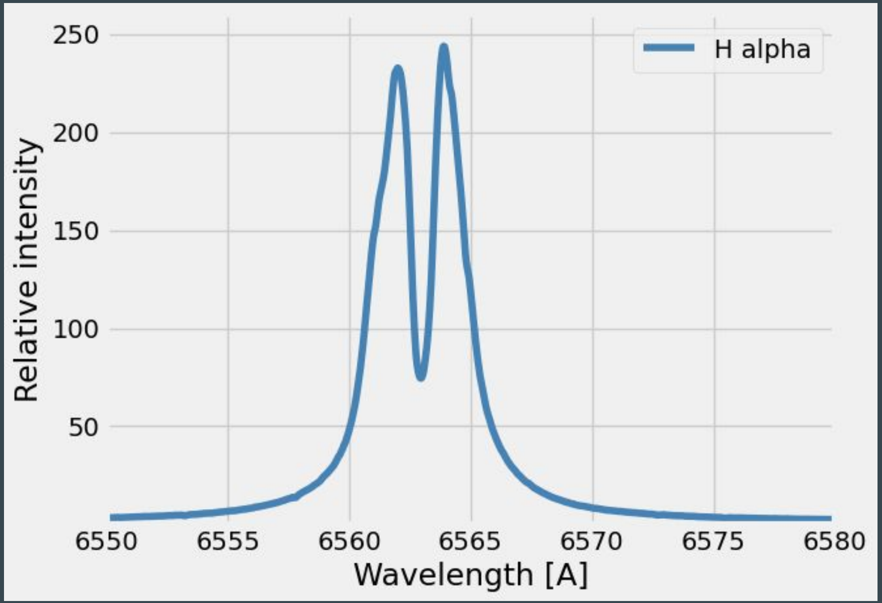

B[e] phenomenon

Strong Balmer emissions

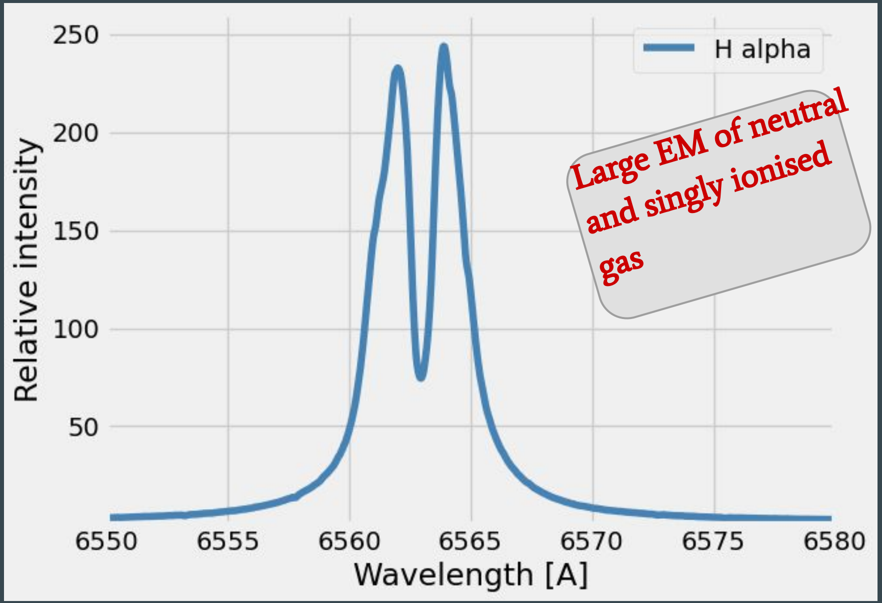

B[e] phenomenon

Strong Balmer emissions

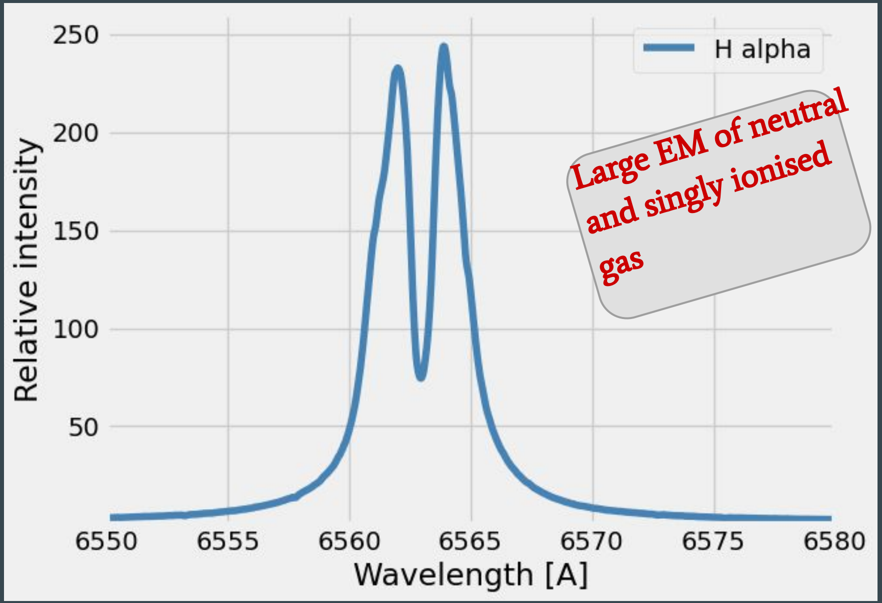

Forbidden emission lines

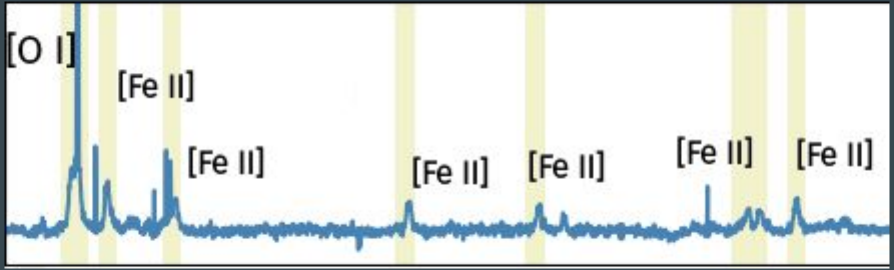

B[e] phenomenon

Strong Balmer emissions

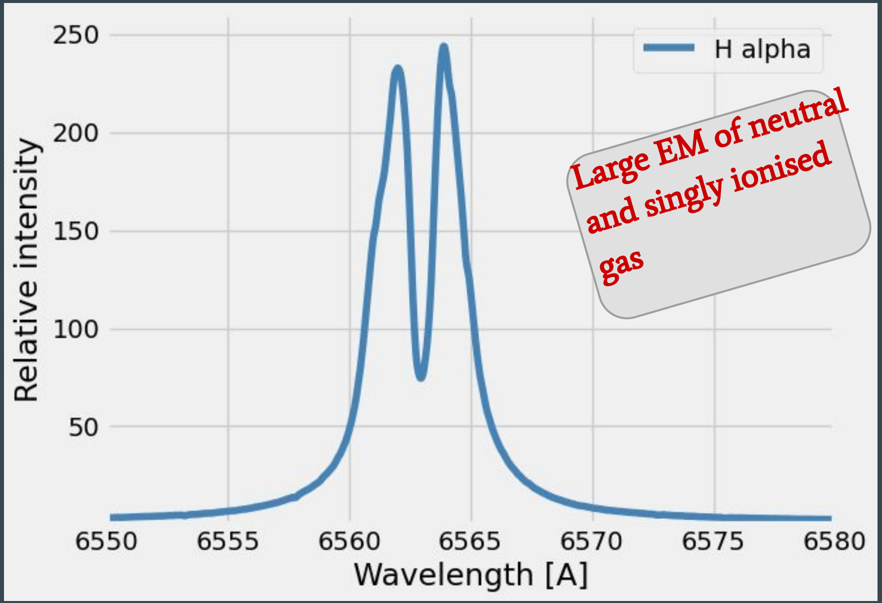

Large EM of neutral and singly ionised gas

Forbidden emission lines

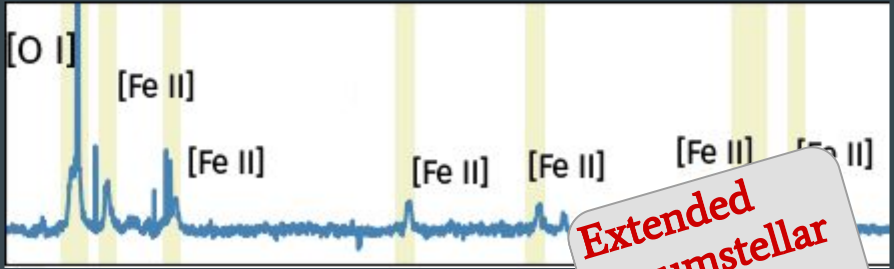

Extended circumstellar envelope

B[e] phenomenon

Strong Balmer emissions

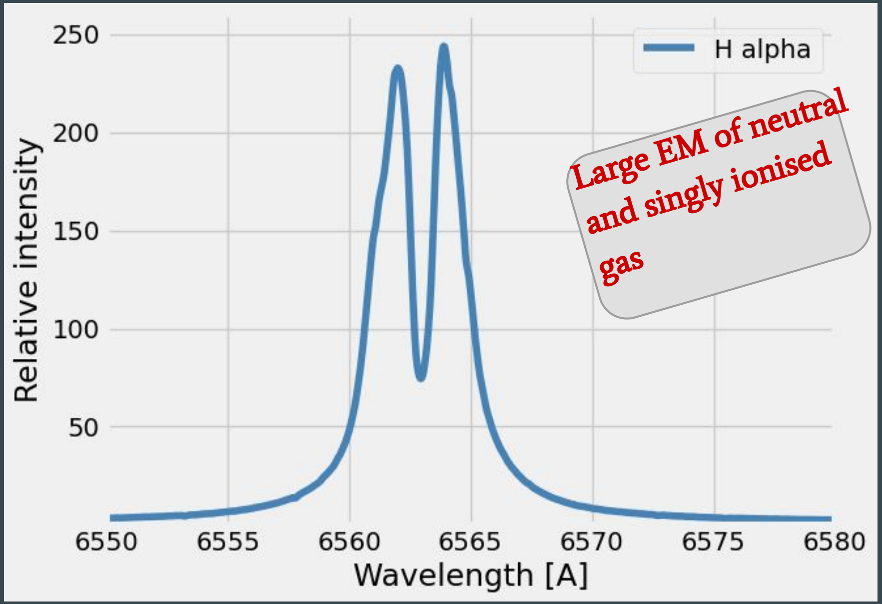

Large EM of neutral and singly ionised gas

Forbidden emission lines

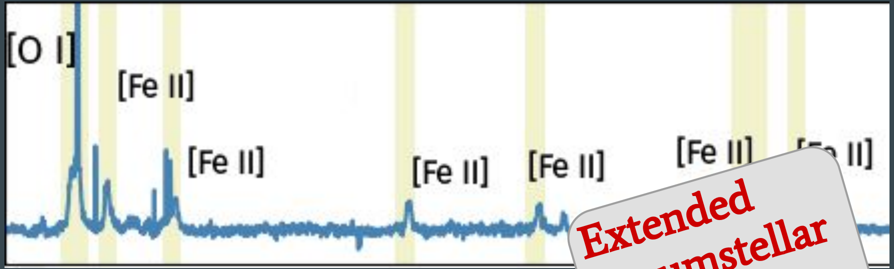

Extended circumstellar envelope

Strong IR excess

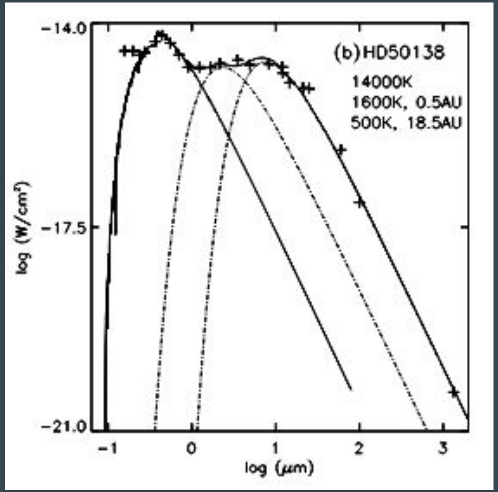

B[e] phenomenon

Strong Balmer emissions

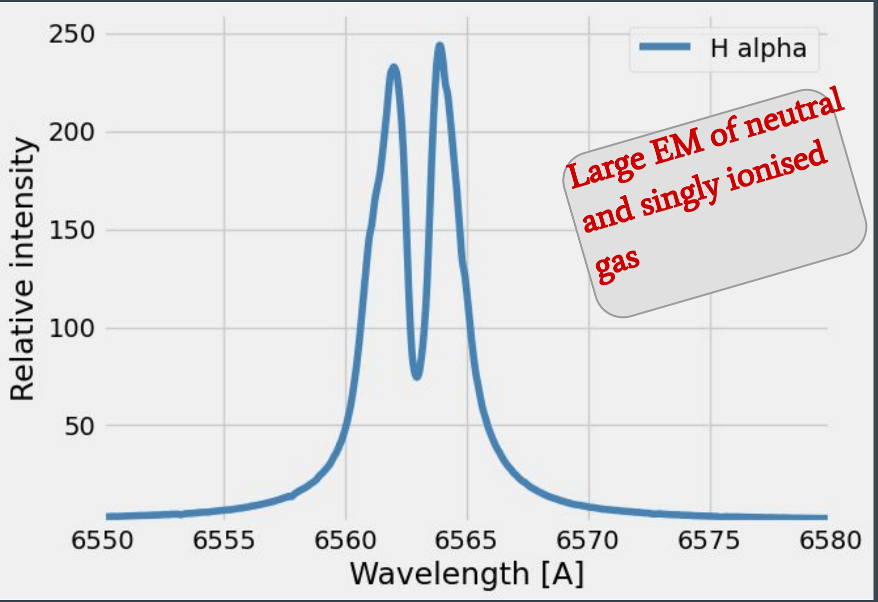

Large EM of neutral and singly ionised gas

Forbidden emission lines

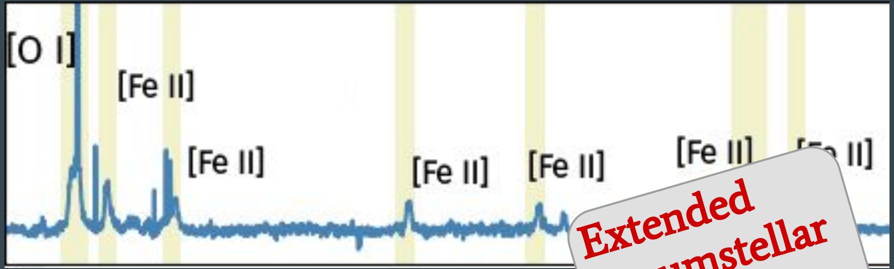

Extended circumstellar envelope

Strong IR excess

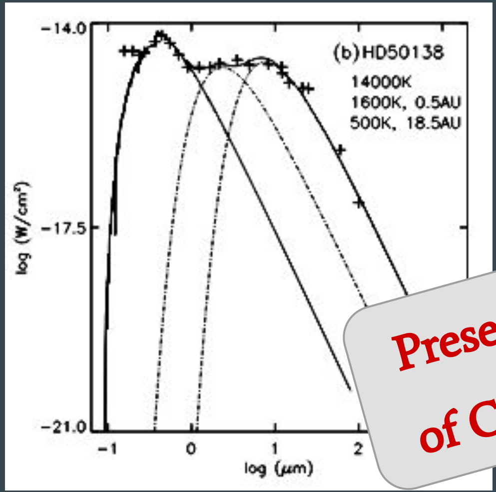

Presence of CS dust

B[e] phenomenon

Strong Balmer emissions

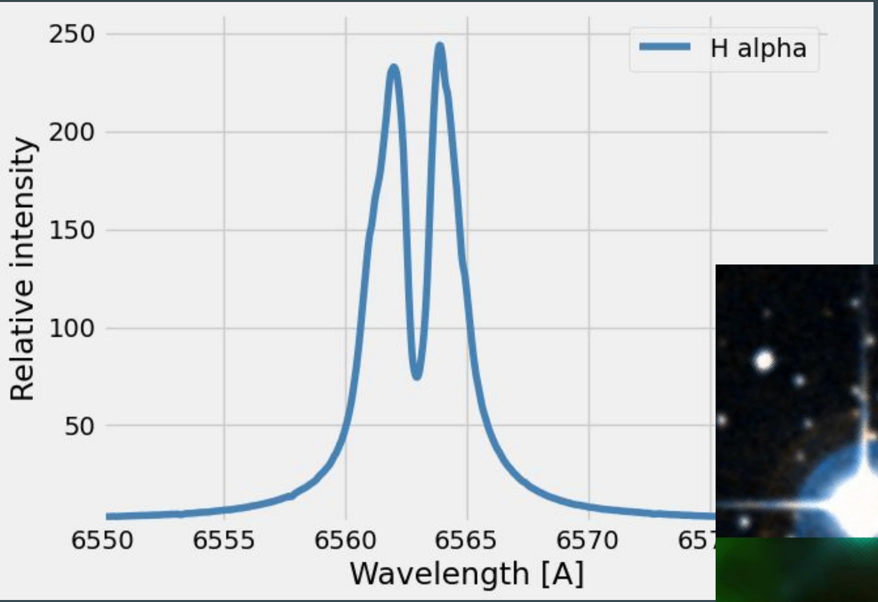

Forbidden emission lines

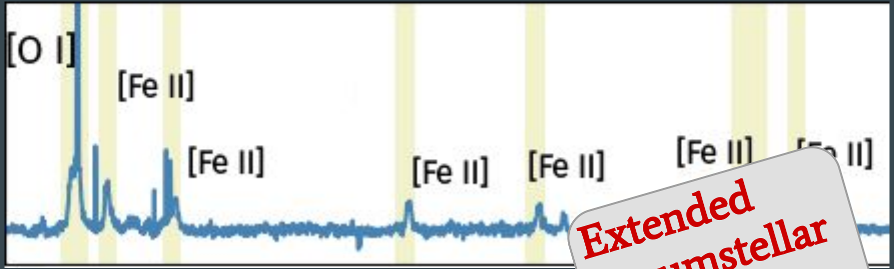

Extended circumstellar envelope

Strong IR excess

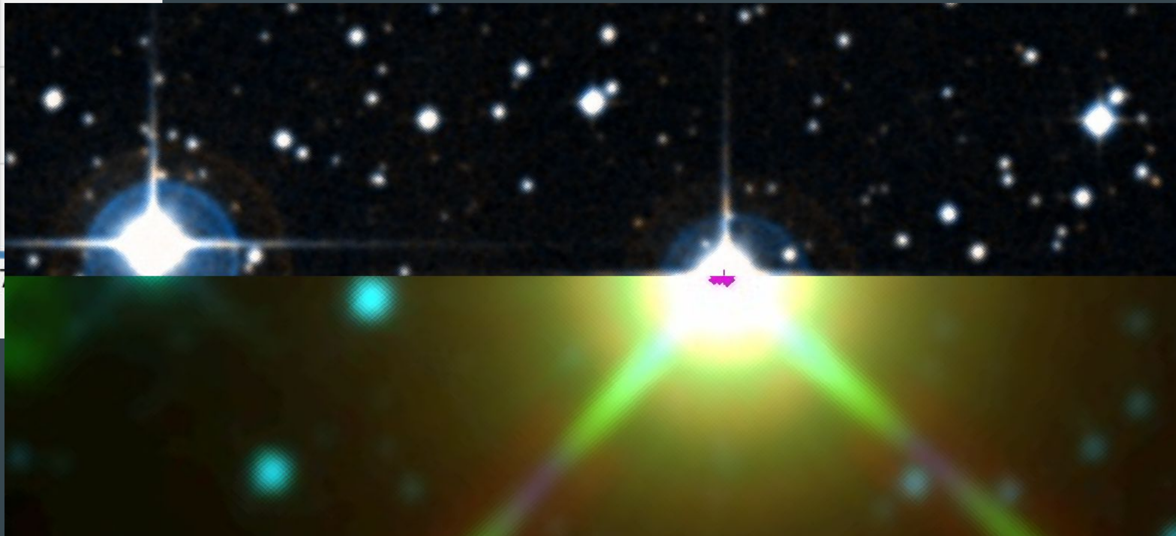

Stars with B[e] phenomenon

Lamers et al. (1998)

Stars with B[e] phenomenon

Lamers et al. (1998)

B[e] supergiants

supergiant -
$\log (L_*/L_\odot) \gtrsim 4.0$

indication of mass loss

hybrid spectra

enhanced N abundances

Stars with B[e] phenomenon

Lamers et al. (1998)

B[e] supergiants

supergiant -
$\log (L_*/L_\odot) \gtrsim 4.0$

indication of mass loss

hybrid spectra

enhanced N abundances

Pre-MS B[e] stars

near star-forming regions, accretion disk

$\log (L_*/L_\odot) \lesssim 4.5$

photometric variations

SED - warm and cool dust

Stars with B[e] phenomenon

Lamers et al. (1998)

B[e] supergiants

supergiant -
$\log (L_*/L_\odot) \gtrapprox 4.0$

indication of mass loss

hybrid spectra

enhanced N abundances

Pre-MS B[e] stars

near star-forming regions, accretion disk

$\log (L_*/L_\odot) \lessapprox 4.5$

photometric variations

SED - warm and cool dust

Compact PN B[e]

spectra show nebula,
$\log (L_*/L_\odot) \lessapprox 4.0$

may show [O III], [S III], [Ne III], ...

may show N enhancement

SED - cold dust (~100K)

Stars with B[e] phenomenon

Lamers et al. (1998)

B[e] supergiants

supergiant -
log $(L_*/L_\odot) \gtrsim 4.0$

indication of mass loss

hybrid spectra

enhanced N abundances

Pre-MS B[e] stars

near star-forming regions, accretion disk

log $(L_*/L_\odot) \lesssim 4.5$

photometric variations

SED - warm and cool dust

Compact PN B[e]

spectra show nebula,
log $(L_*/L_\odot) \lesssim 4.0$

may show [O III], [S III], [Ne III], ...

may show N enhancement

SED - cold dust (~100K)

Symbiotic B[e] stars

evidence of a cool companion in the spectrum (TiO band)

late-type spectrum in near IR

Stars with B[e] phenomenon

Lamers et al. (1998)

B[e] supergiants

supergiant -
log $(L_*/L_\odot) \gtrsim 4.0$

indication of mass loss

hybrid spectra

enhanced N abundances

Pre-MS B[e] stars

near star-forming regions, accretion disk

log $(L_*/L_\odot) \lesssim 4.5$

photometric variations

SED - warm and cool dust

Compact PN B[e]

spectra show nebula, log $(L_*/L_\odot) \lesssim 4.0$

may show [O III], [S III], [Ne III], ...

may show N enhancement

SED - cold dust (~100K)

Symbiotic B[e] stars

evidence of a cool companion in the spectrum (TiO band)

late-type spectrum in near IR

Unclassified B[e] stars

-> do not fit

HD 45677, HD 50138 or HD 87643, ...

FS CMa stars

FS CMa stars - definition from Miroshnichenko 2007

Emission-line spectra contains: Balmer lines, Fe II, [O I], ([Fe II], weak [O III])

IR excess - peak at 10 - 30 μm

Location outside of star-forming regions

If companion - fainter and cooler than primary (degenarate)

-> primary T = 9 000 - 30 000 K

-> $(L_*/L_\odot)$ between 2.5 and 4.5

Observed properties

Photometry

- chaotic behavior (multiperiodicity)
- pulsations, co-rotating structures, dust occultations, material infall, material ejecta, wind, moving layers

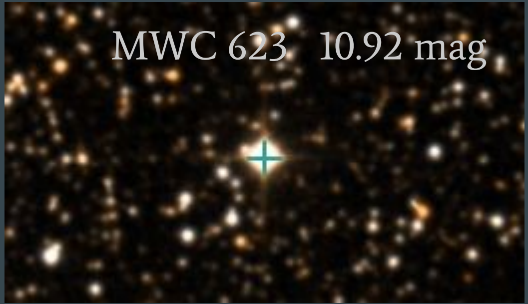

Observed properties

Photometry

- chaotic behavior (multiperiodicity)
- pulsations, co-rotating structures, dust occultations, material infall, material ejecta, wind, moving layers

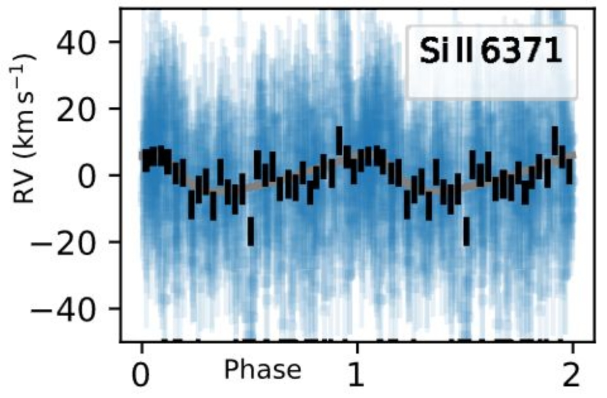

GG Car, 1.583 d period, Porter et al. (2012a)

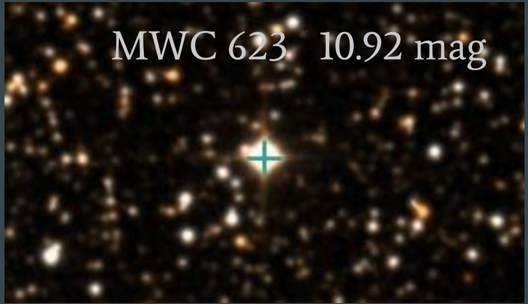

Observed properties

Spectral variability

- **absorption lines** - night to night
- **emission lines** - weeks to months
- **forbidden lines** - months to years

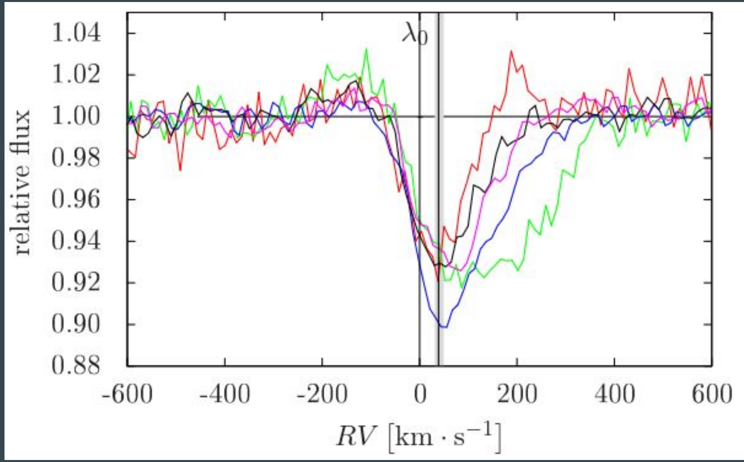

HD 50138, He I 6678 Å, Jeřábková et al. (2016)

Observed properties

Spectral variability

- **absorption lines** - night to night
- **emission lines** - weeks to months
- **forbidden lines** - months to years

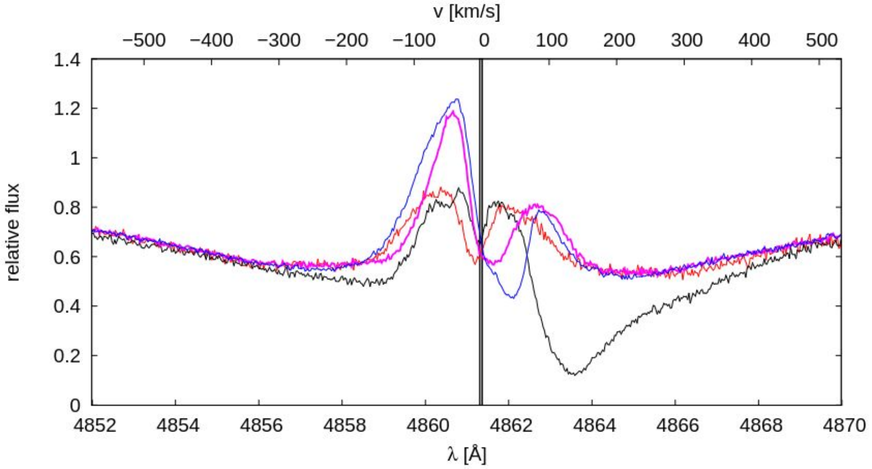

IRAS 17449+2320, Korčáková (2022)

Observed properties

Spectral variability

- absorption lines - night to night
- emission lines - weeks to months
- forbidden lines - months to years

Various features may be observed

- dusty clumps, material infall or ejecta

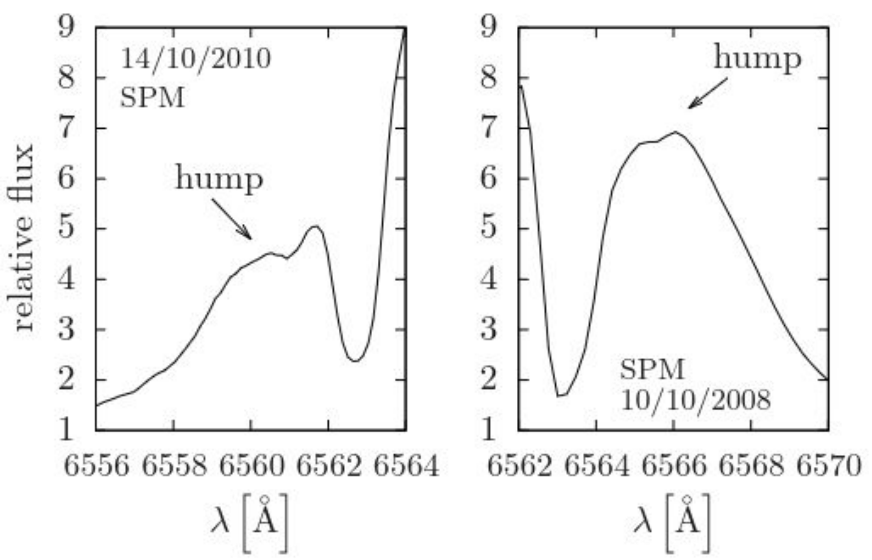

HD 50138, Jeřábková et al. (2016)

Observed properties

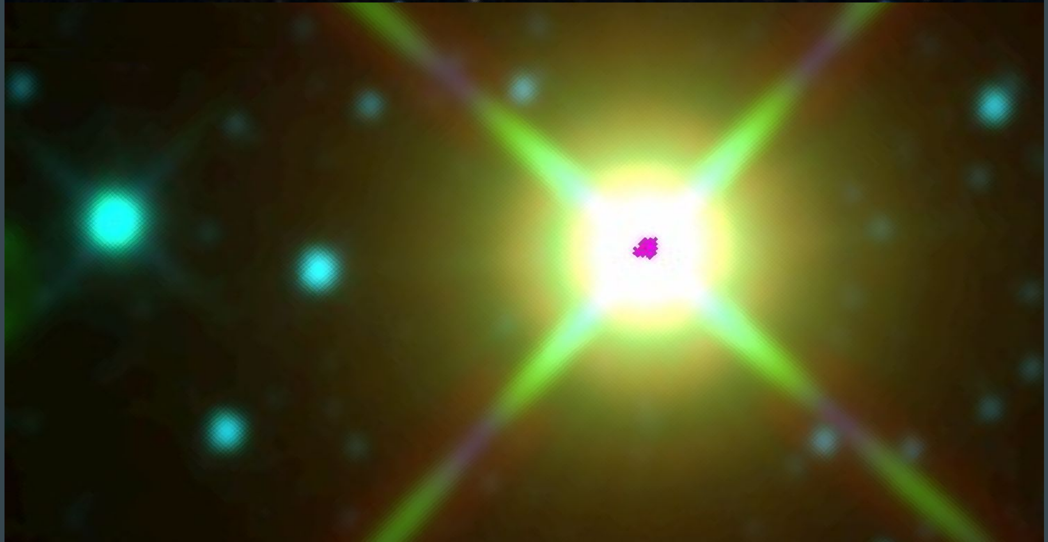

Observed properties

Systems with ongoing or finished dust formation

Strong mass loss in at least two cases (HD 87643, AS 78)

$10^{-6}\ M_\odot/\mathrm{yr}$

Higher than can be explained by radiatively driven wind

-> Stellar evolution of a single star is not enough

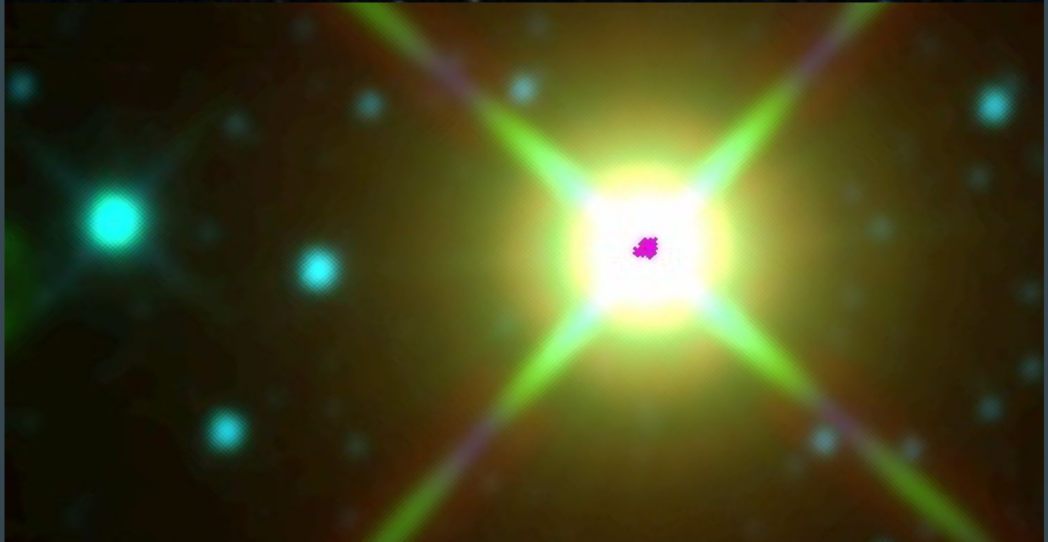

Binary hypothesis

Miroshnichenko 2007

-> binaries with mass transfer

- K-type companion (**MWC 623** and **V669 Cep**)
- degenerate comp. (**CI Cam**)
- brightness variations attributed to orbital motion (**AS 160** and **MWC 342**)
- spectro-astrometry (**FS CMa**, **HD 50138**, and **HD 85567**)

Binary hypothesis

Miroshnichenko 2007

-> binaries with mass transfer

- K-type companion (**MWC 623** and **V669 Cep**)
- degenerate comp. (**CI Cam**)
- brightness variations attributed to orbital motion (**AS 160** and **MWC 342**)
- spectro-astrometry (**FS CMa**, **HD 50138**, and **HD 85567**)

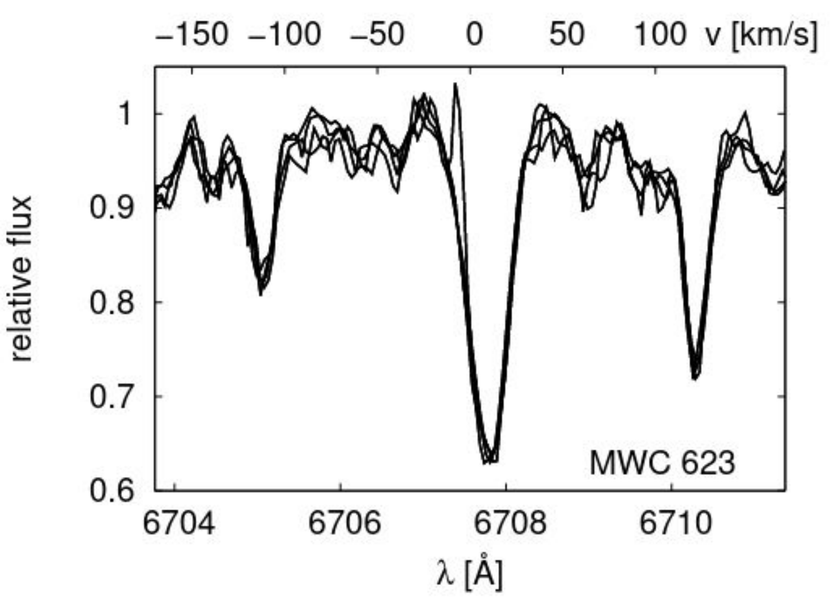

Korčáková et al. (2020)

Interferometric observations

Presence of dust - most likely in a disk around the star

Interplay of many processes

- puffed-up rim due to dust sublimation
- dusty halo, dusty wind
- **near IR instruments**

Interferometric observations

Presence of dust - most likely in a disk around the star

Interplay of many processes

- puffed-up rim due to dust sublimation
- dusty halo, dusty wind
- **near IR instruments**

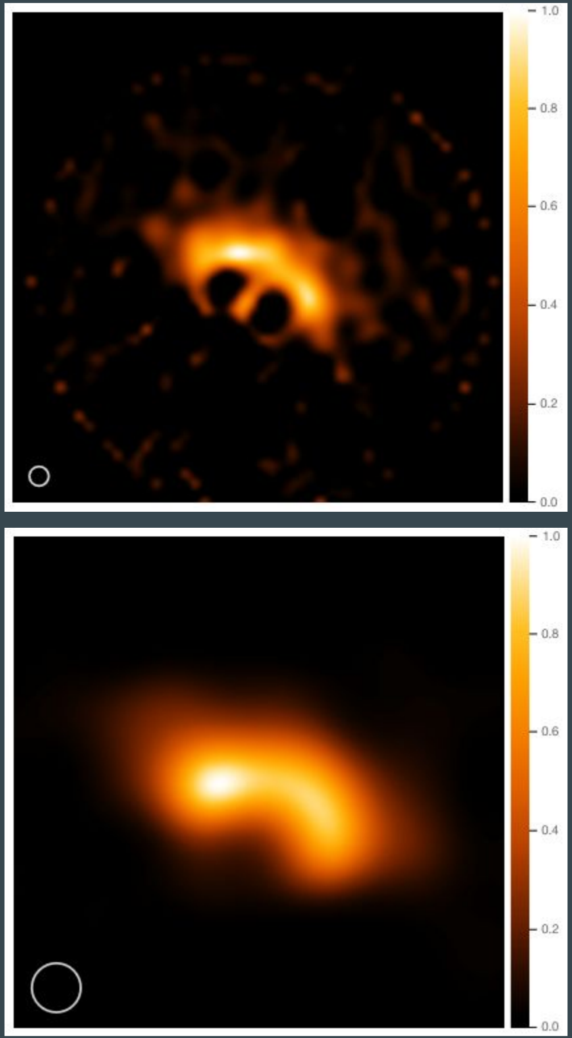

Hofmann et al. (2022), FS CMa

Interferometric observations

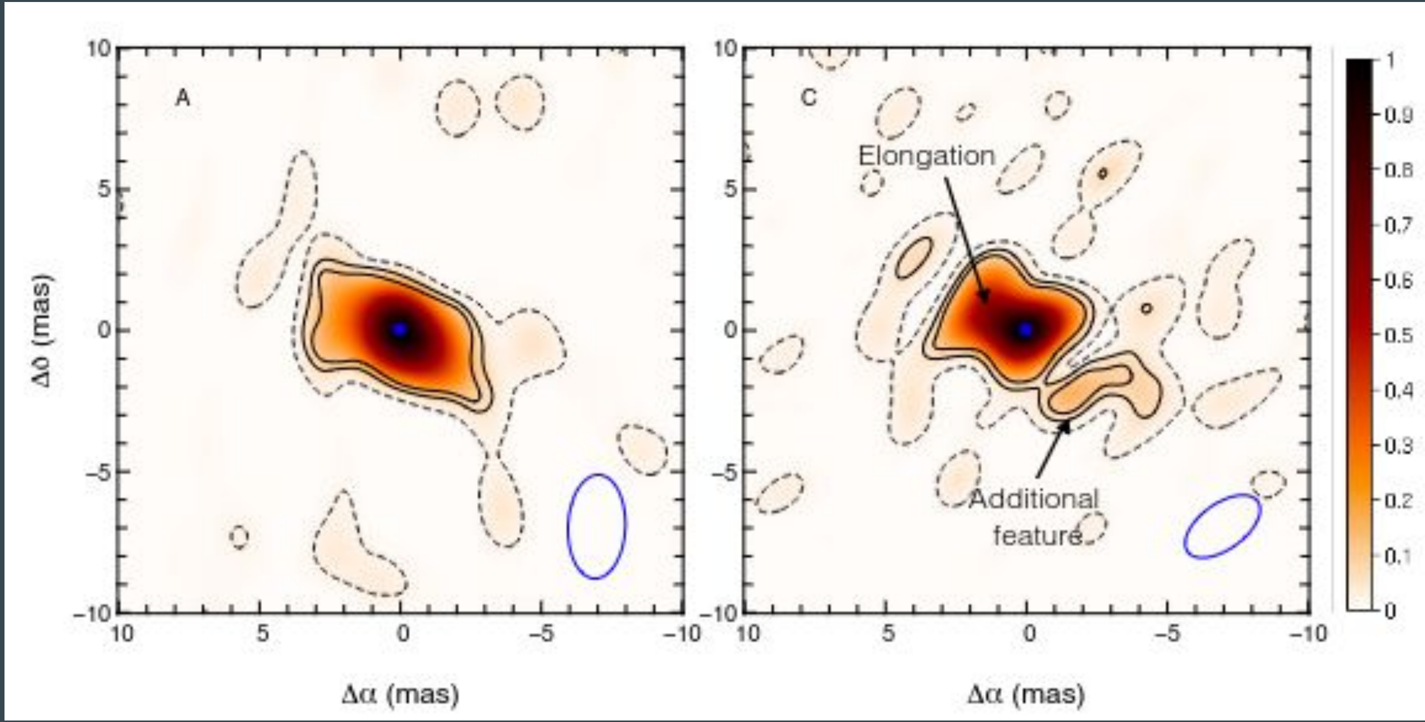

HD 50138, Kluska et al. 2016

Magnetic field discovered!

Strong magnetic field found for the first time in a FS CMa

(Korčáková et al. 2022)

IRAS 17449+2320

6.2 ± 0.2 kG

Strong Zeeman split in many spectral lines

Magnetic field discovered!

Strong magnetic field found for the first time in a FS CMa

(Korčáková et al. 2022)

IRAS 17449+2320

6.2 ± 0.2 kG

Strong Zeeman split in many spectral lines

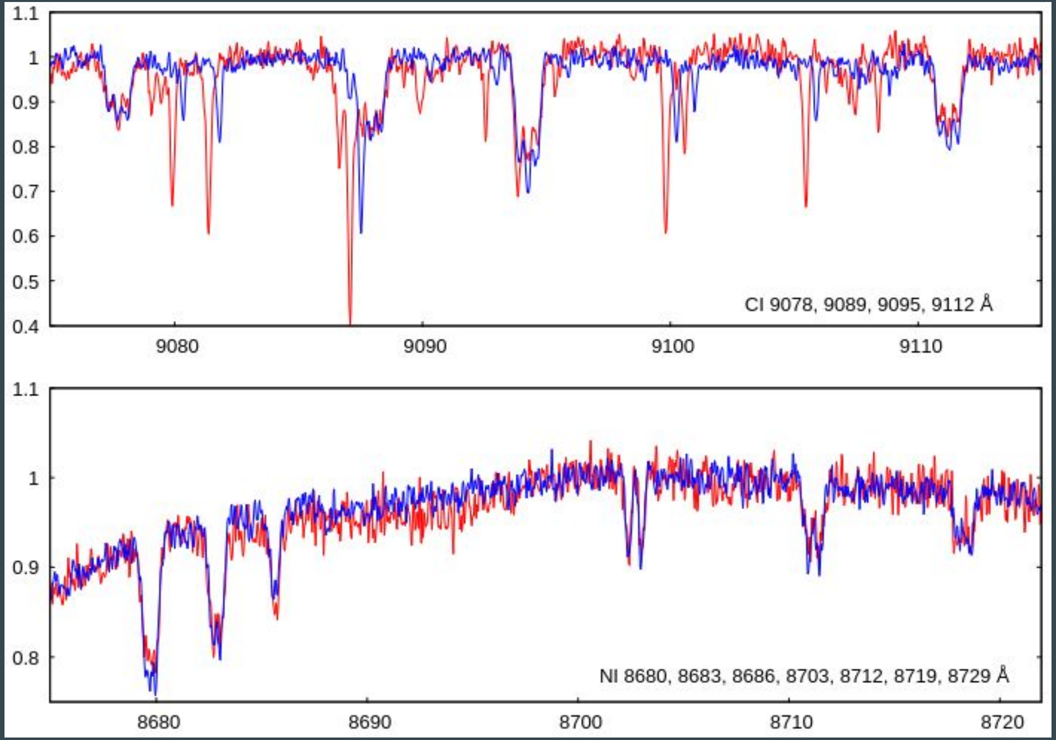

Korčáková et al. 2022

New hypothesis

Strong magnetic field

Slow rotation

Appearance of young stellar objects, but far from star forming regions

Position on the HR diagram near TAMS

Large space velocities

New hypothesis

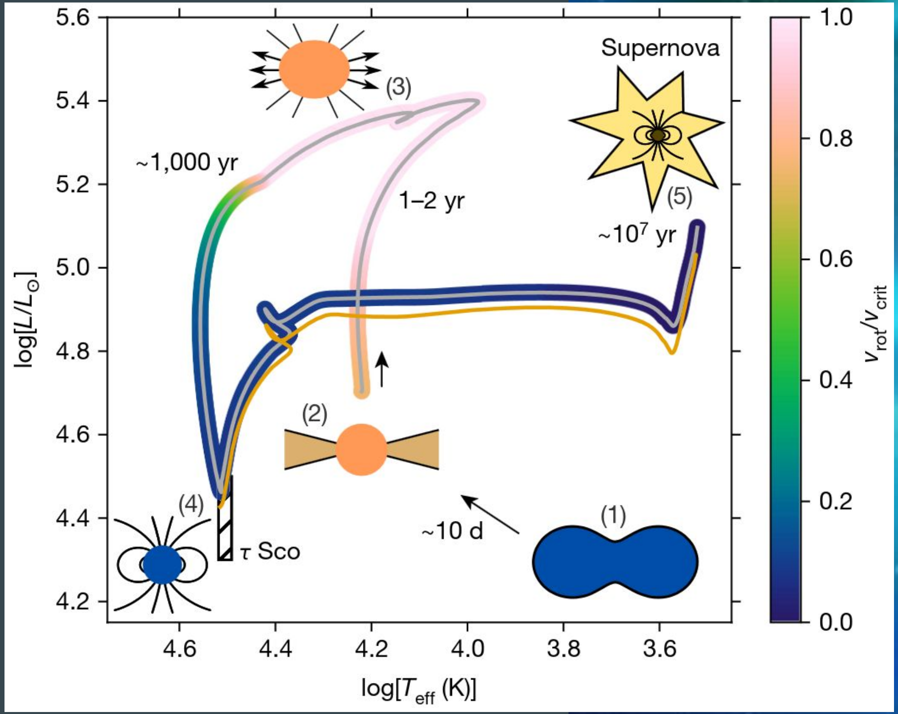

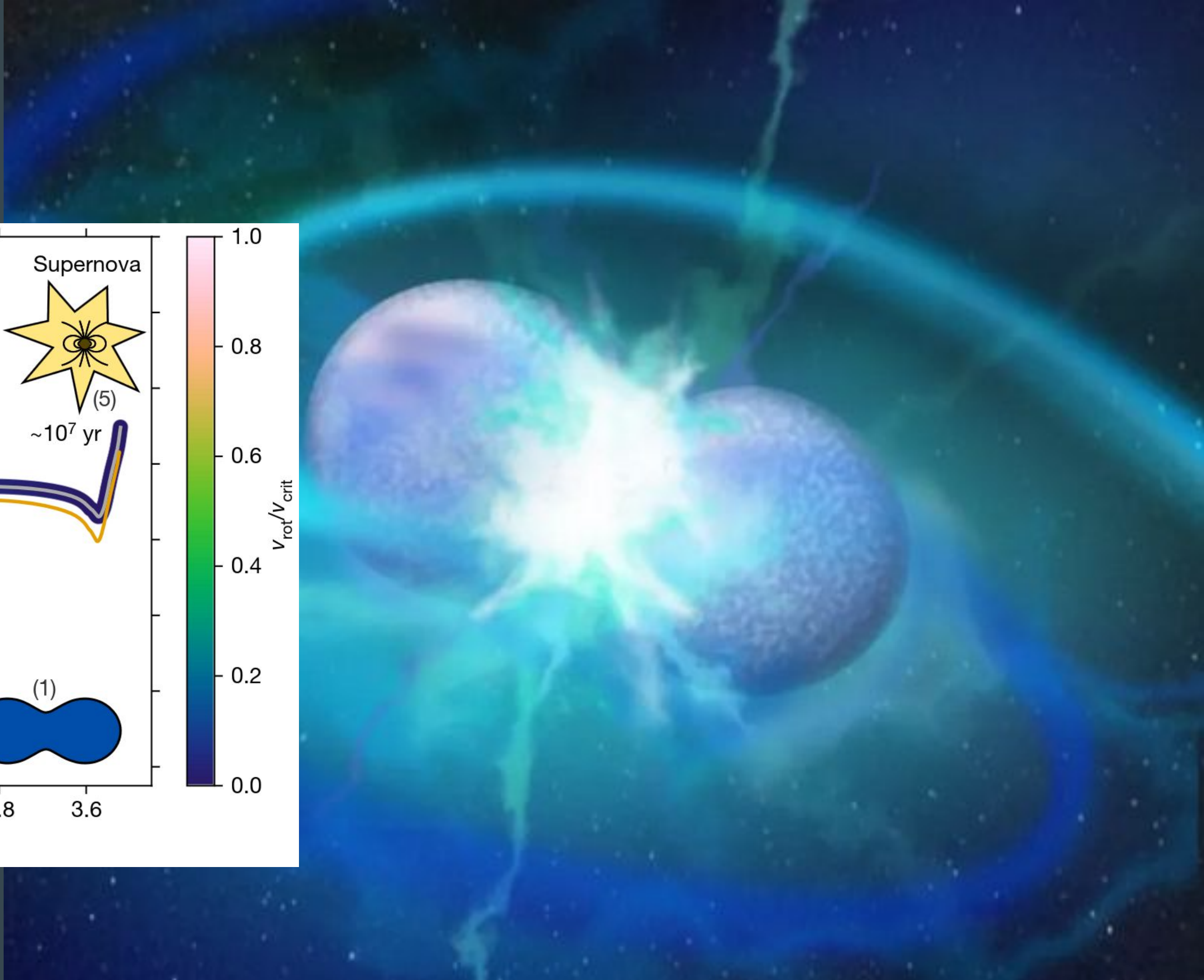

Schneider et al. 2020

New hypothesis

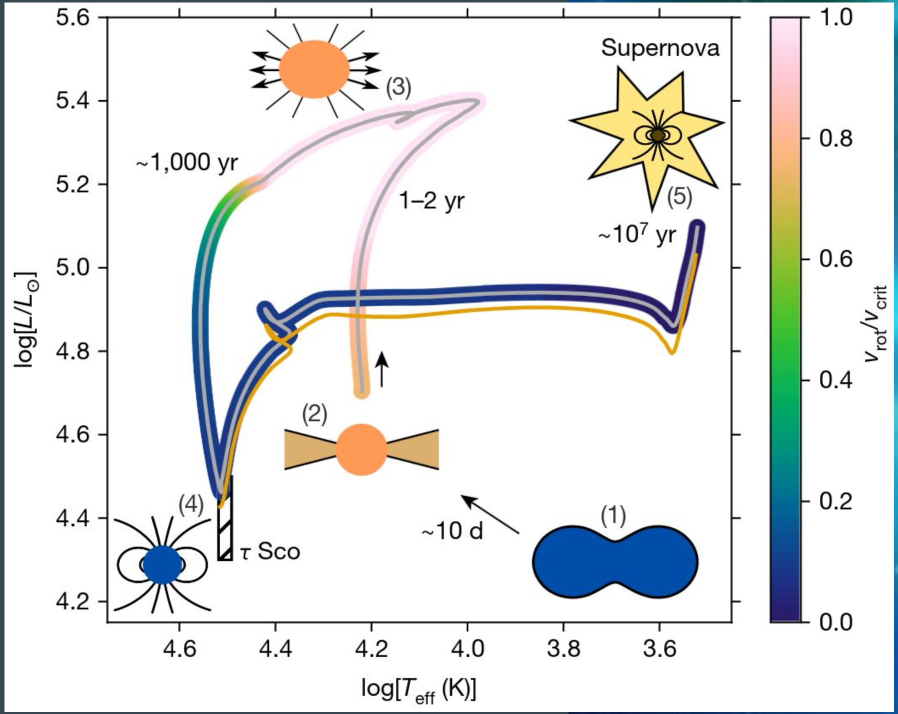

Schneider et al. 2020

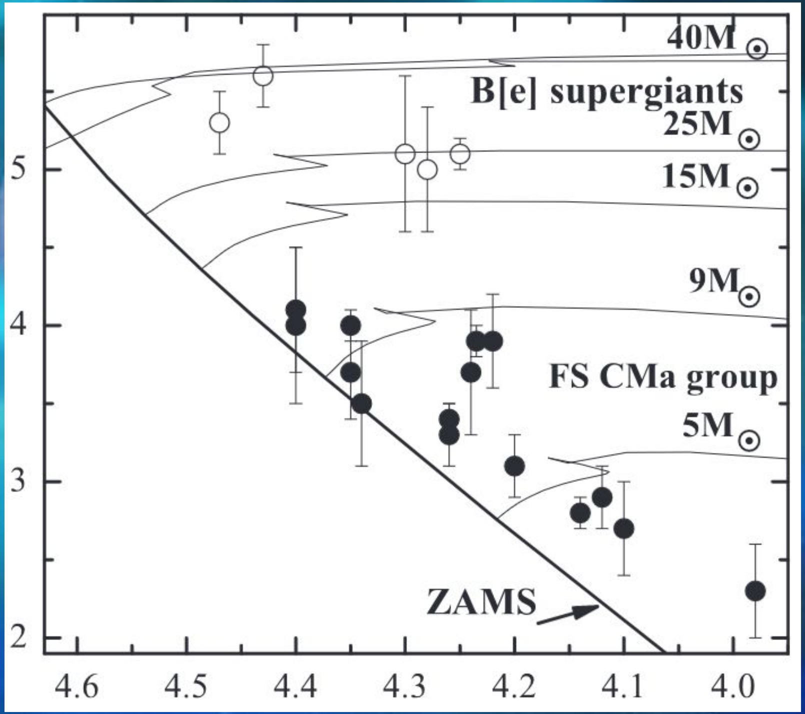

Miroshnichenko et al. 2017

N-body simulations

NBODY6 code

Open clusters in galactic potential, 8.5 kpc from Galactic center

$M[M_\odot] \approx$	8000	4100	2040	1030	510	255	130	62
# simulations	2	4	8	16	32	64	128	256
# stars per cluster ≈	13 680	7070	3590	1860	980	510	260	140

Sp.type	$M\ [M_\odot]$
O	> 16
B	2.1 - 16
A	1.4 - 2.1
F	1.04 - 1.4
G	0.8 - 1.04
K	0.45 - 0.8
M	0.08 - 0.45
BrDw	< 0.08

statistical study - focus on mergers - distribution of spectral types

Initial orbital period distribution with a threshold mass 2 $M_\odot$ and 5 $M_\odot$

...

Dvořáková N., Korčáková D., Dinnbier F. and Kroupa P. (submitted)

N-body simulations

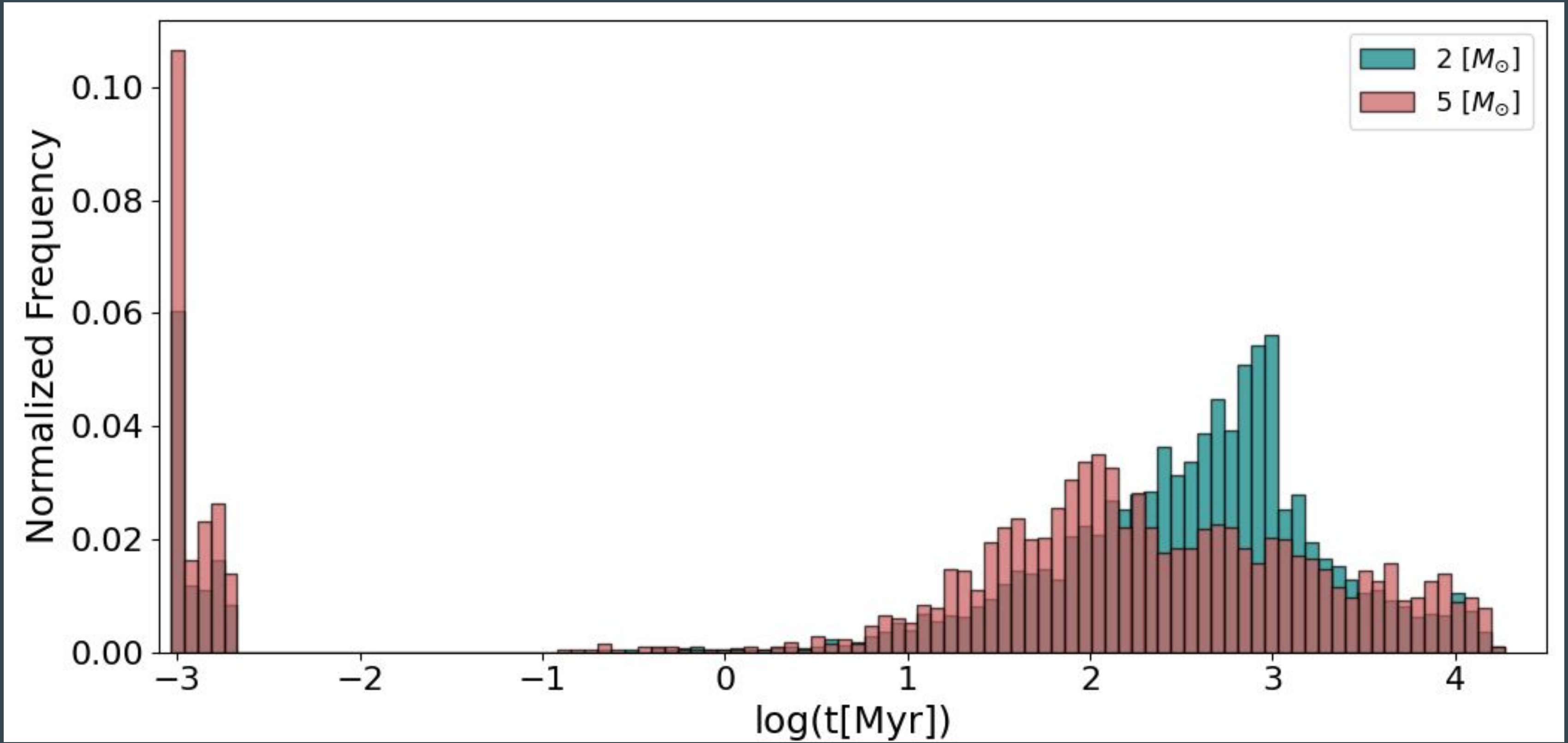

N-body simulations

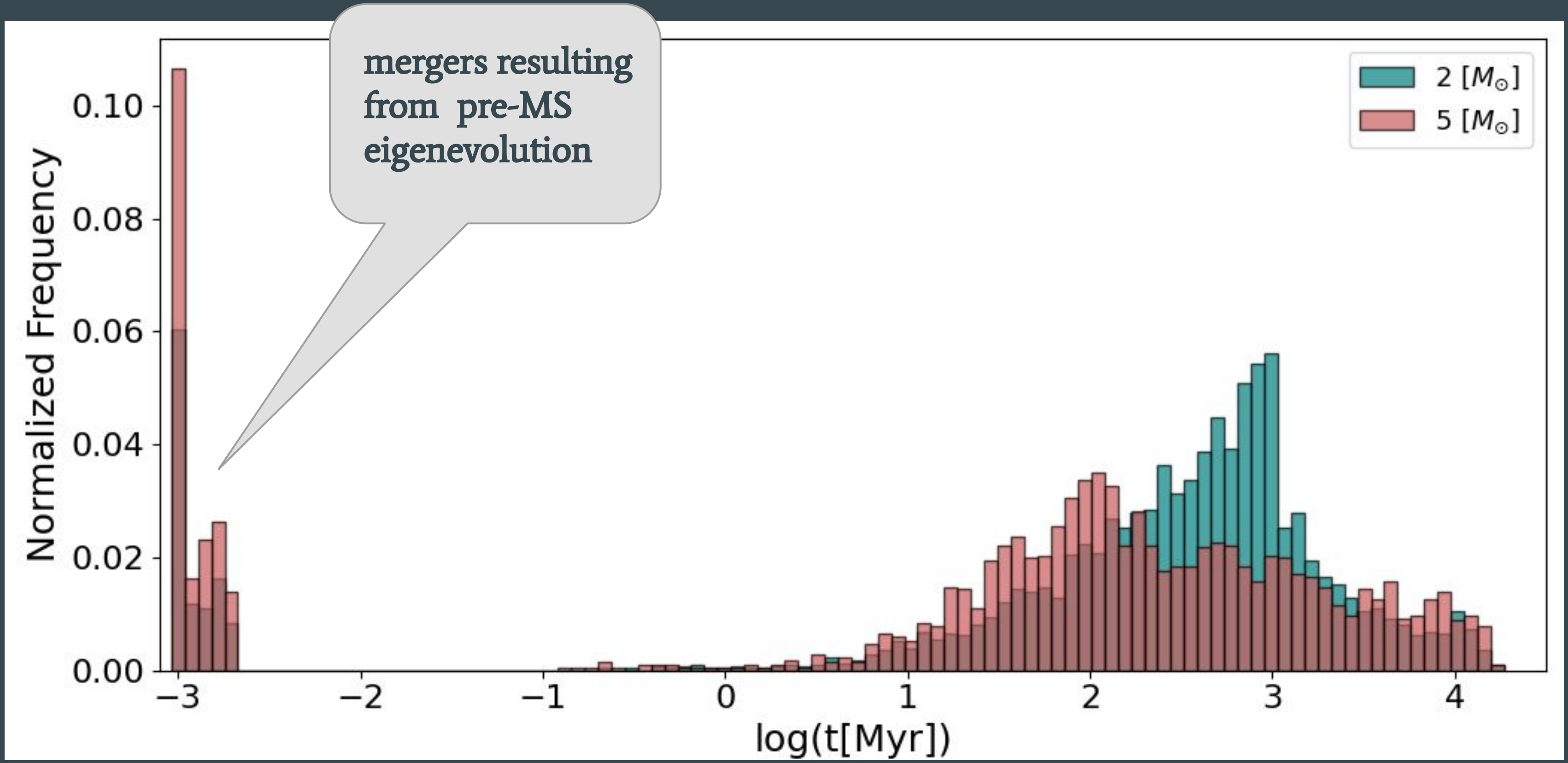

N-body simulations

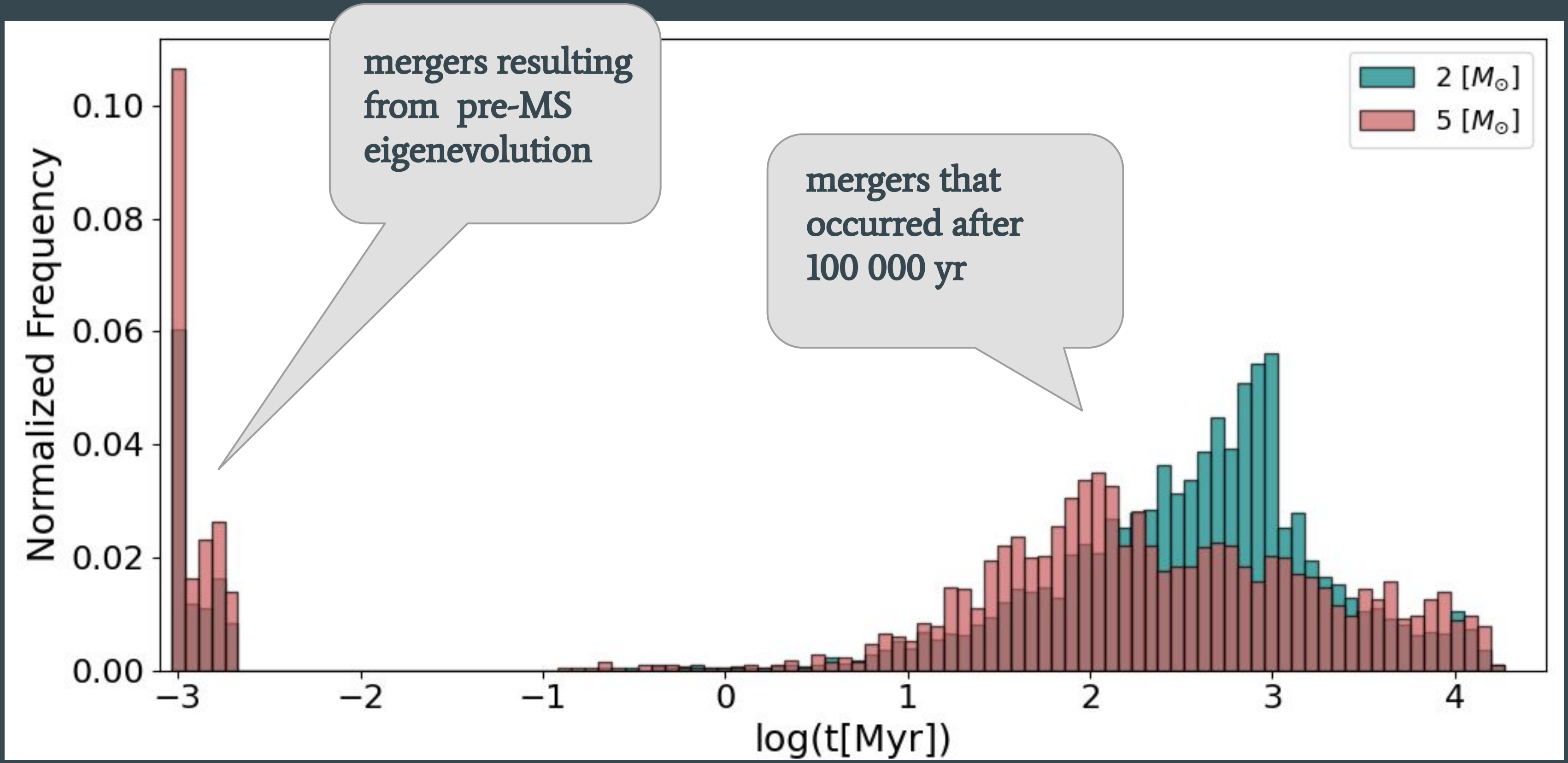

N-body simulations

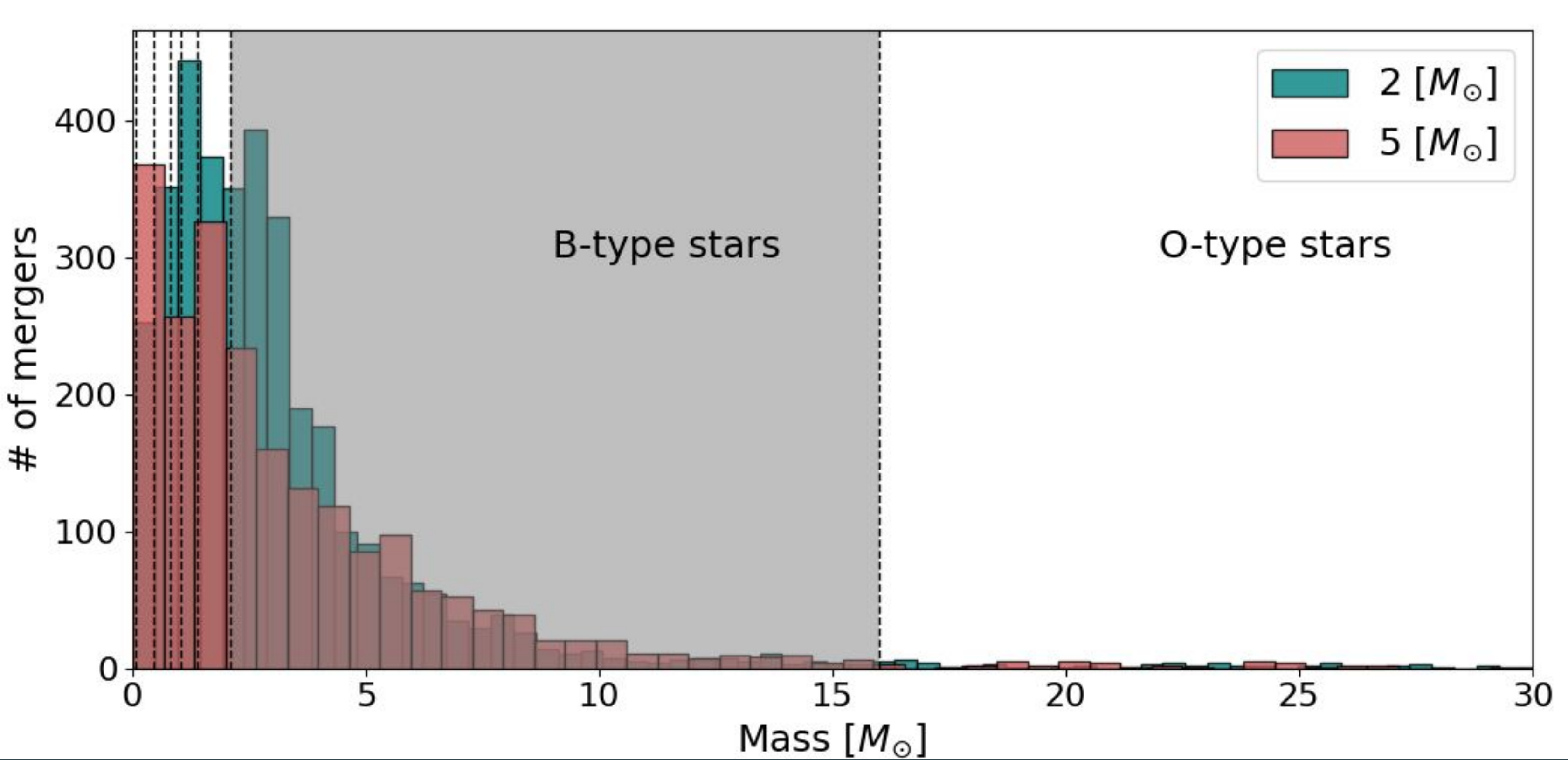

N-body simulations - more than 50% of mergers are B stars

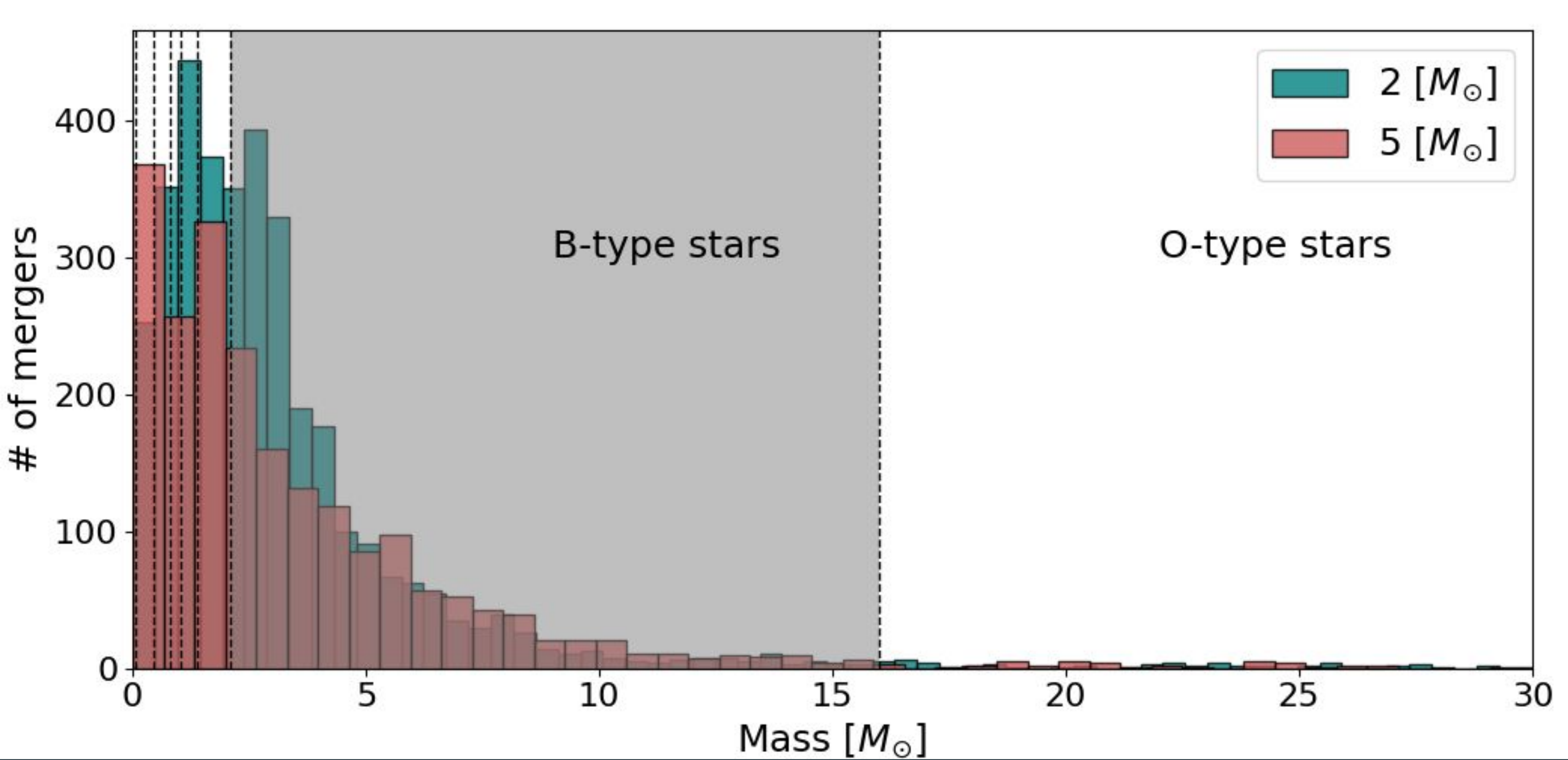

N-body simulations - around 15 % of mergers - A stars

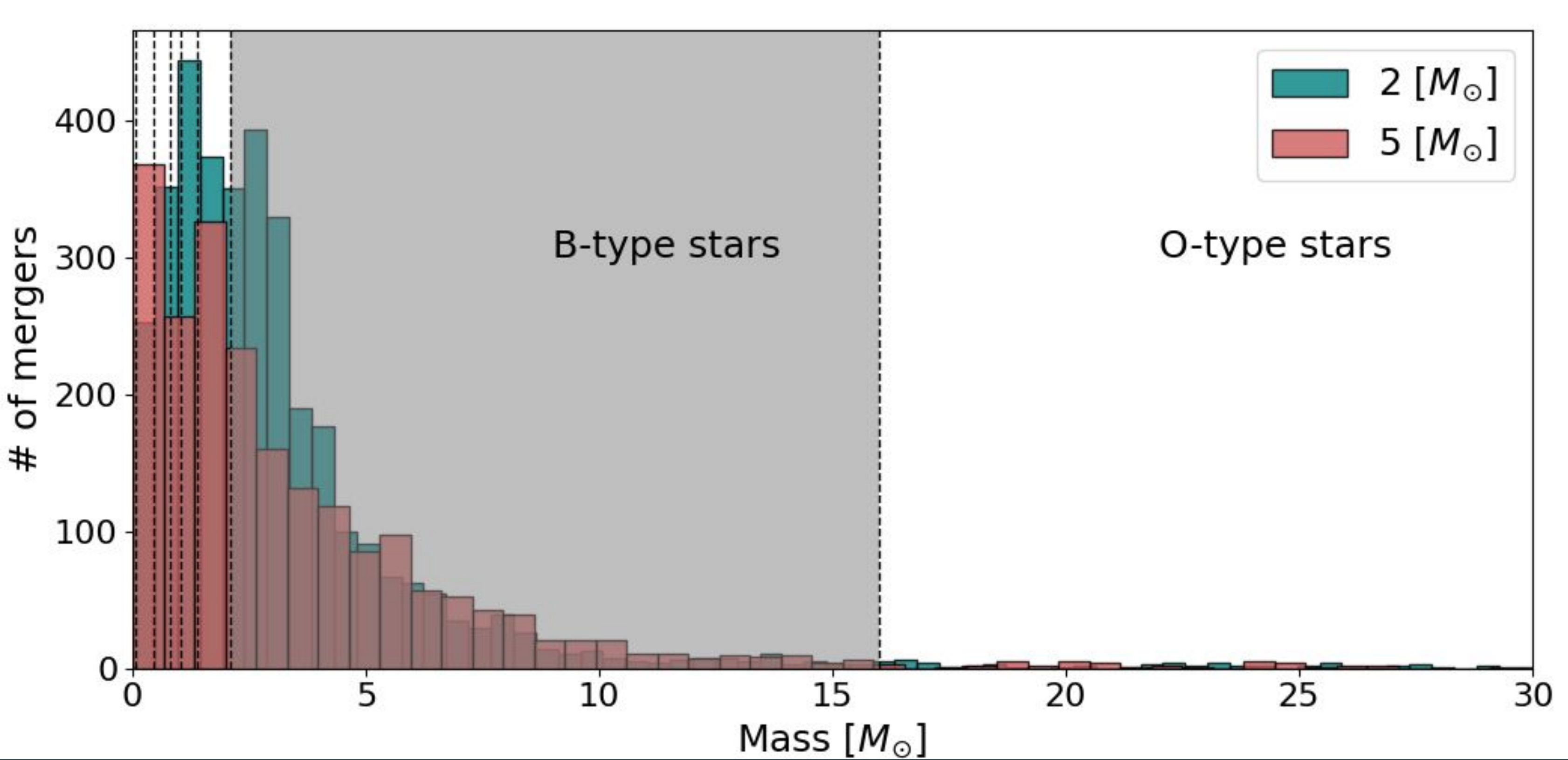

N-body simulations

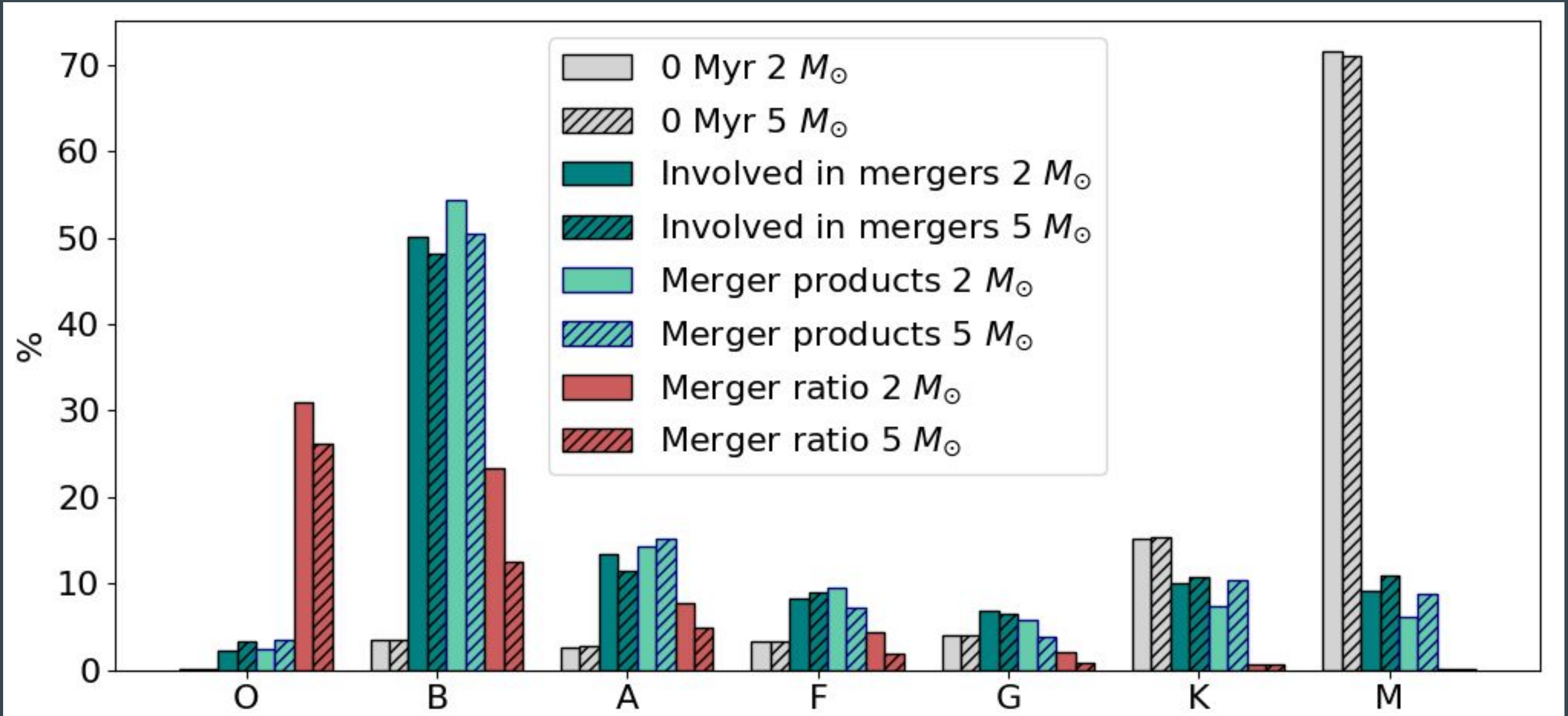

N-body simulations

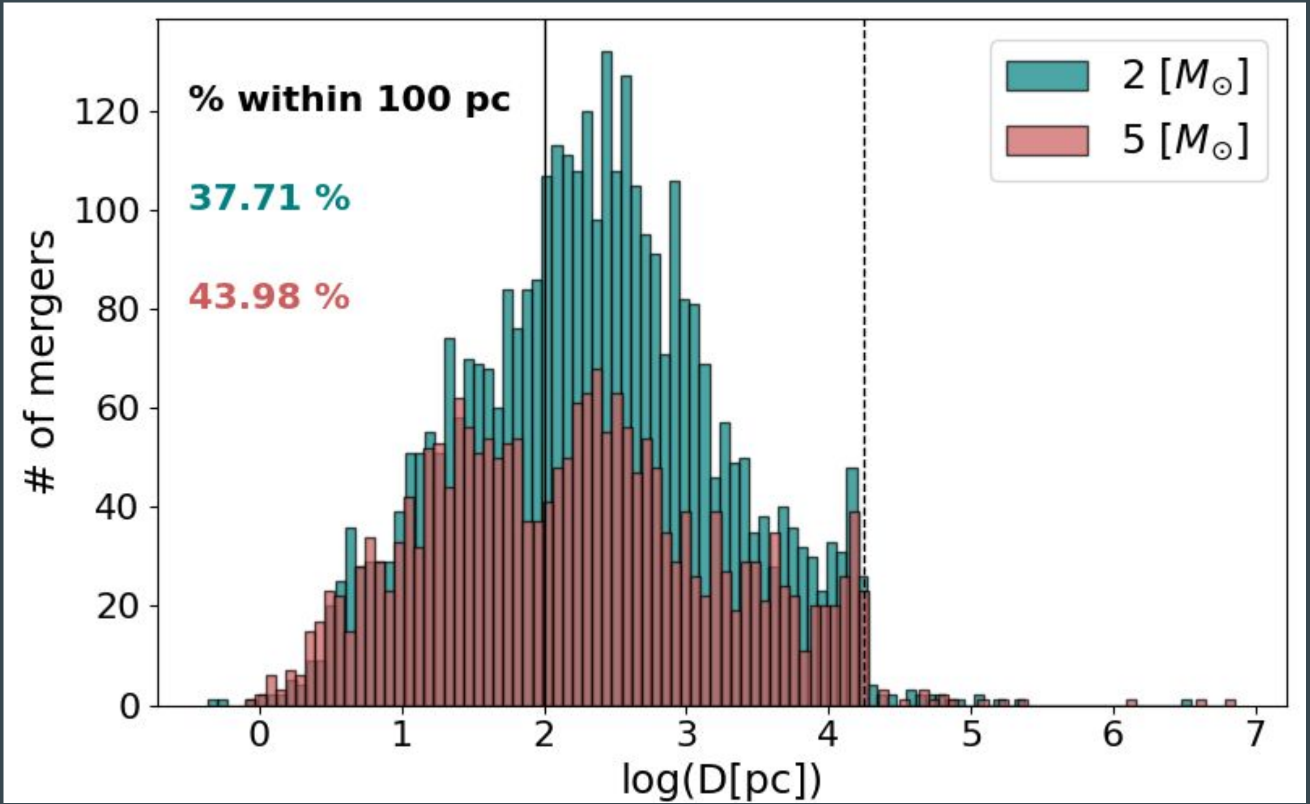

N-body simulations

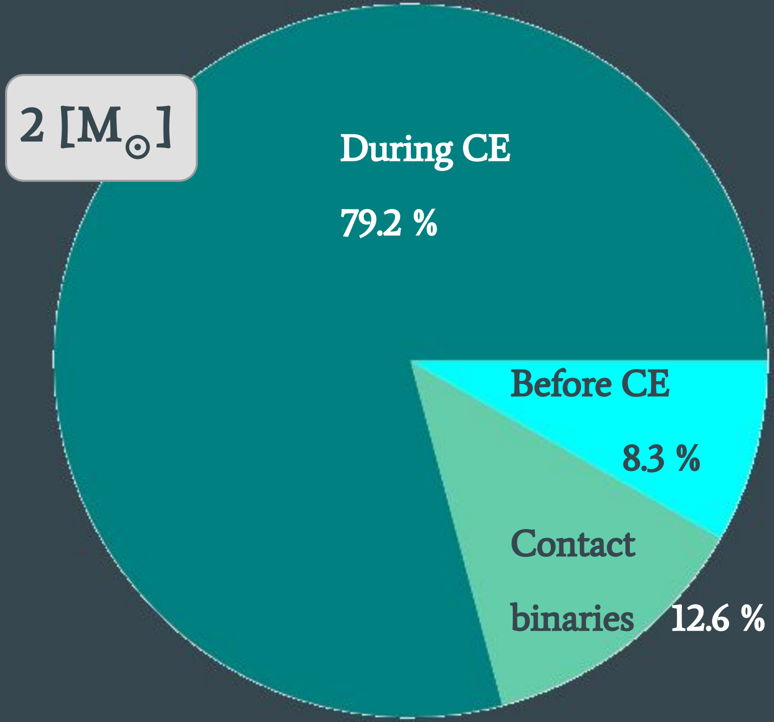

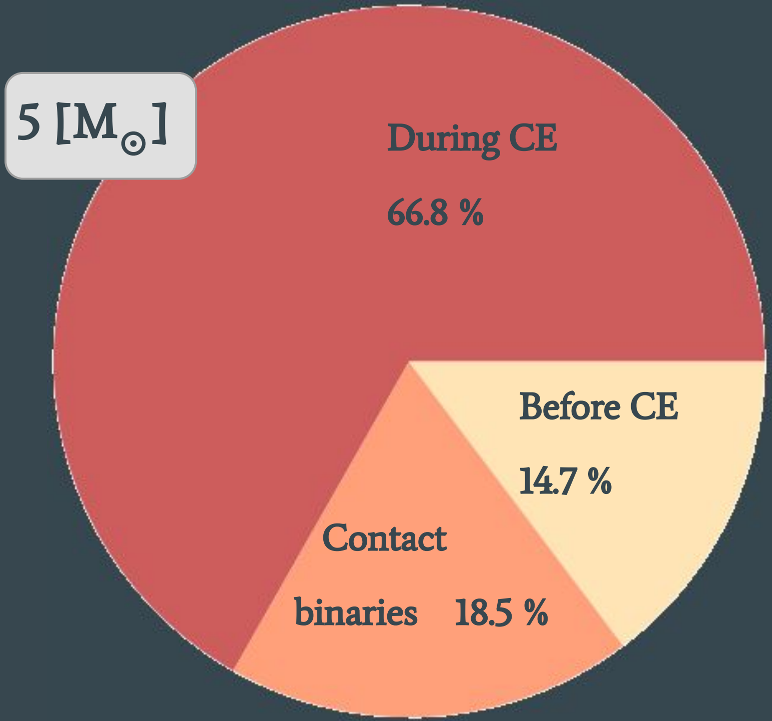

N-body simulations

- Interaction with a third star
- binary kicked out
- short semi-major axis and a large eccentricity
- tidal circularisation
- possibly a merger

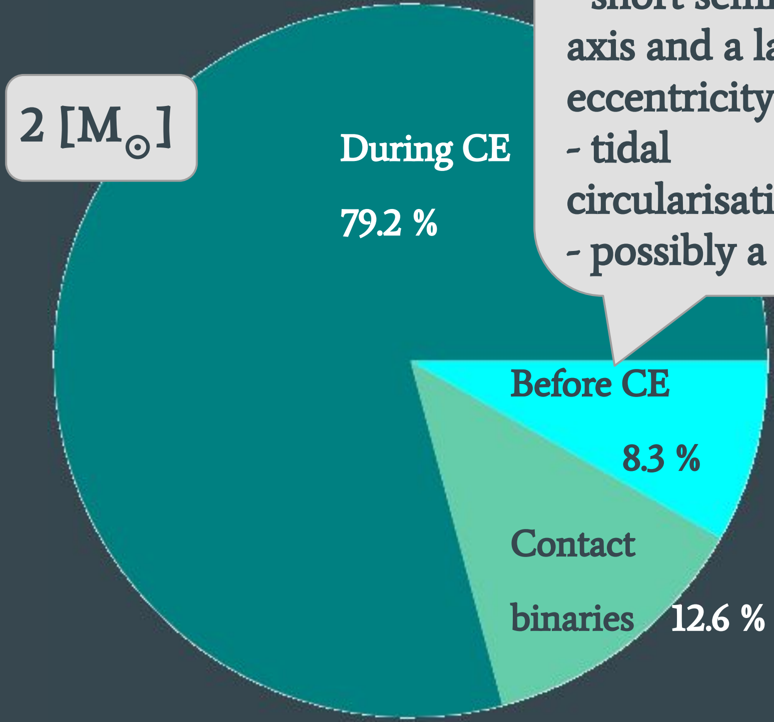

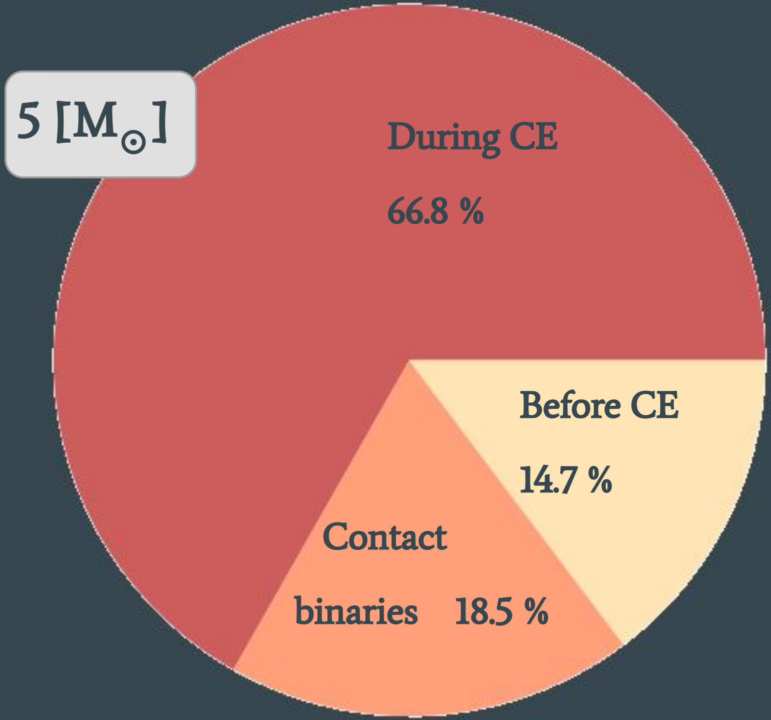

N-body simulations

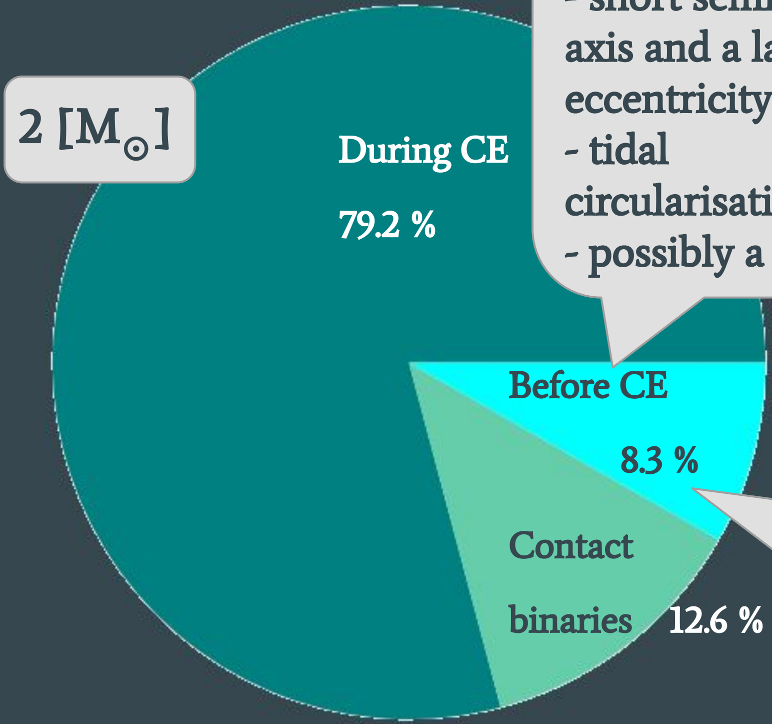

- Interaction with a third star
- binary kicked out
- short semi-major axis and a large eccentricity
- tidal circularisation
- possibly a merger

Also due to stellar evolution

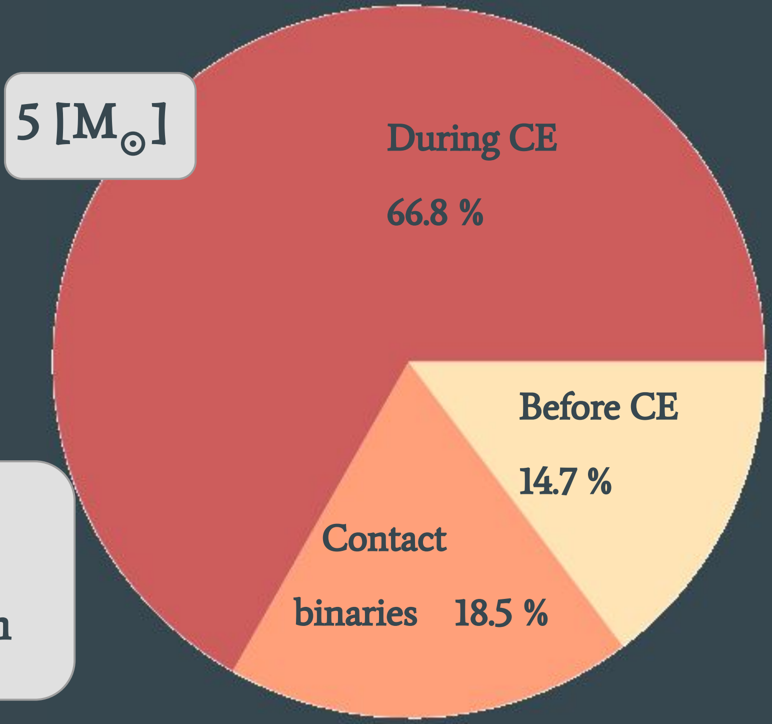

N-body simulations

2 $[M_\odot]$

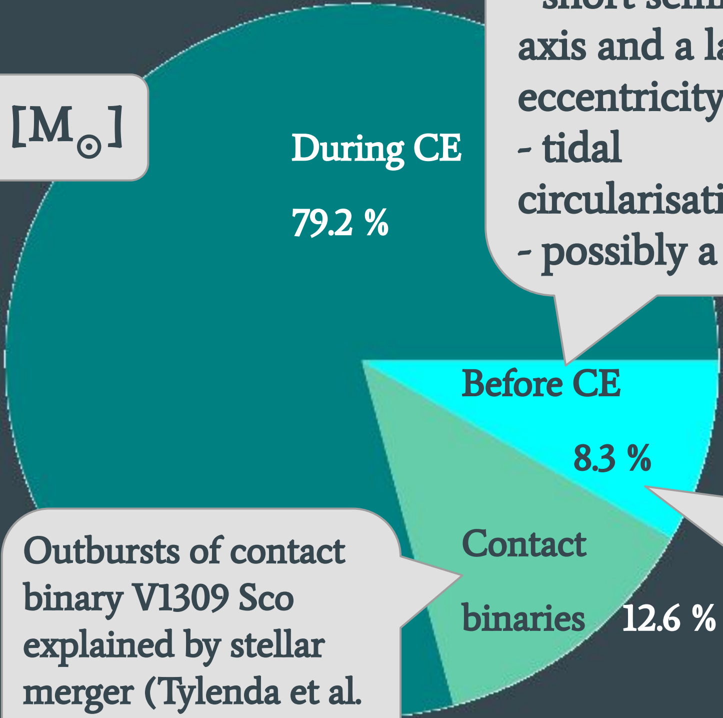

- Interaction with a third star
- binary kicked out
- short semi-major axis and a large eccentricity
- tidal circularisation
- possibly a merger

Also due to stellar evolution

Outbursts of contact binary V1309 Sco explained by stellar merger (Tylenda et al. 2011)

5 $[M_\odot]$

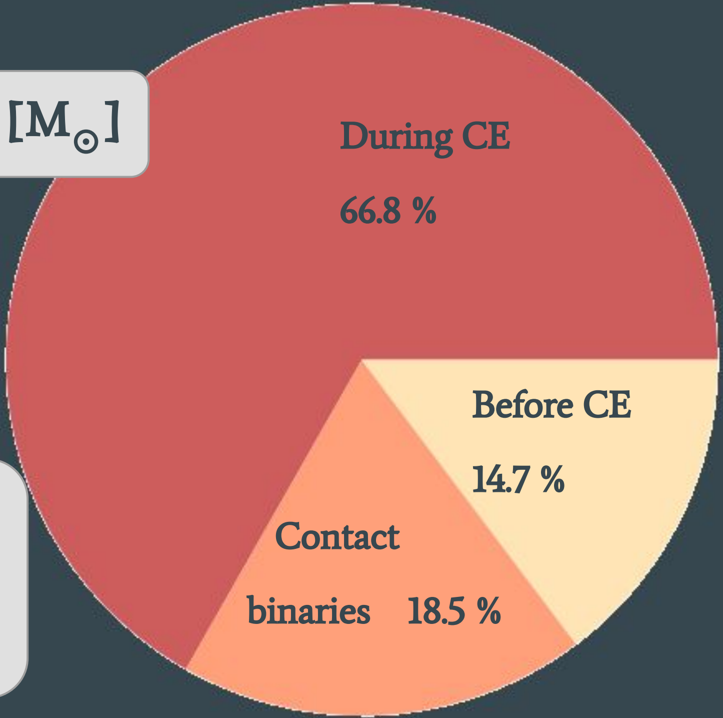

Comparison with observations

Rv measurements for 32 FS CMa stars
- [O I] 6300.304, 6363.776 Å

GAIA data

-> **space velocities**

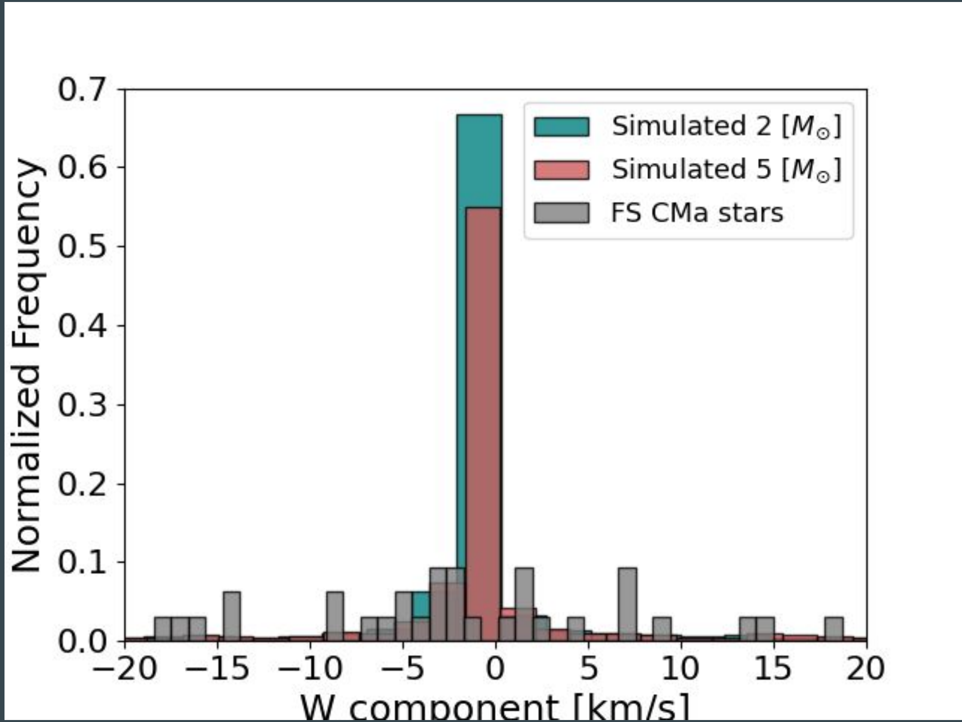

Comparison with observations

Rv measurements for 32 FS CMa stars
- [O I] 6300.304, 6363.776 Å

GAIA data

-> **space velocities**

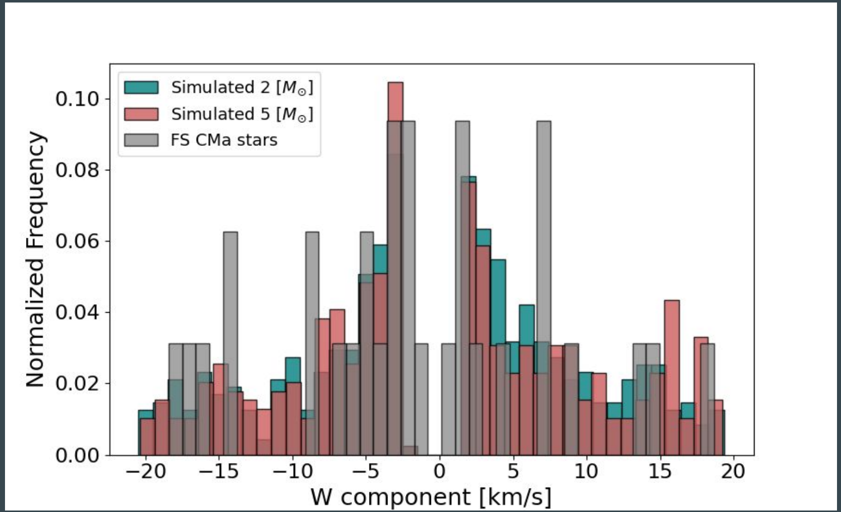

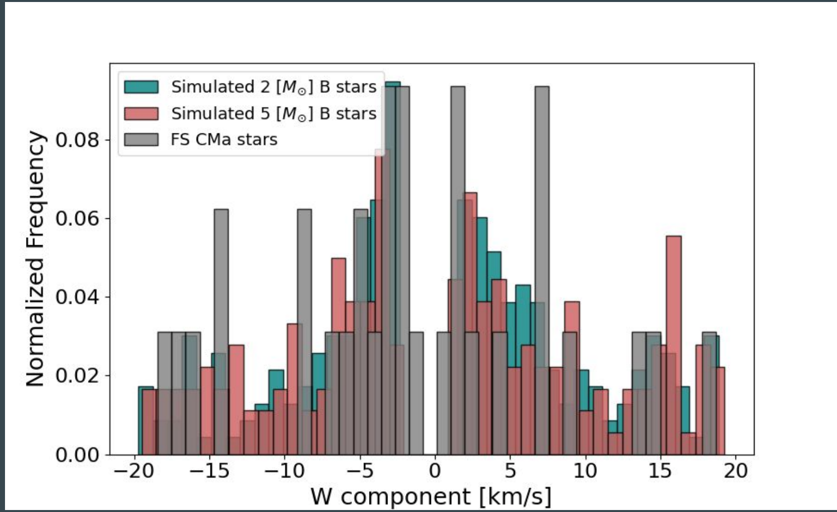

Current view of FS CMa stars

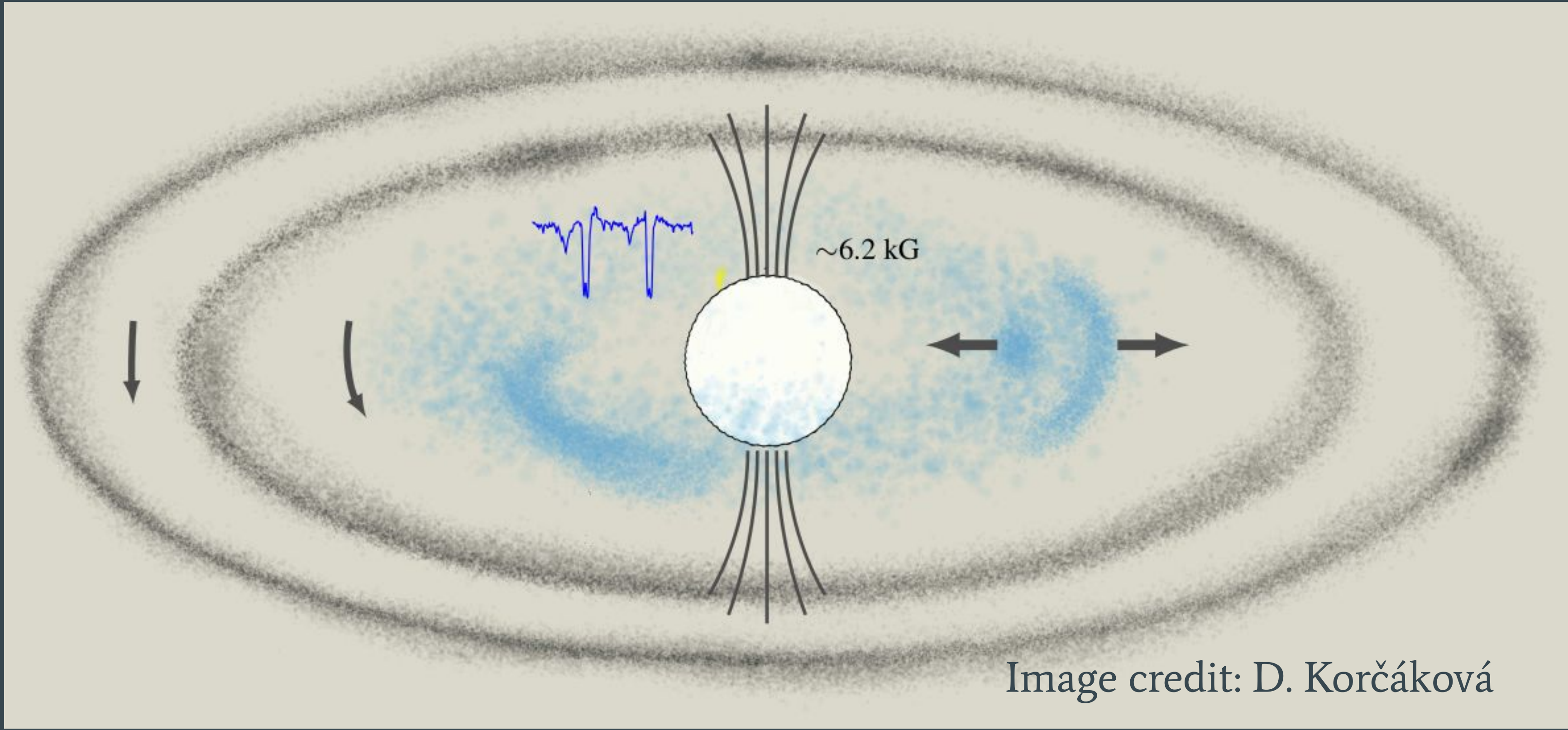

Conclusions

FS CMa stars - **OVERLOOKED CHANNEL OF STELLAR MERGERS**

Merger events are dominated by B-type stars

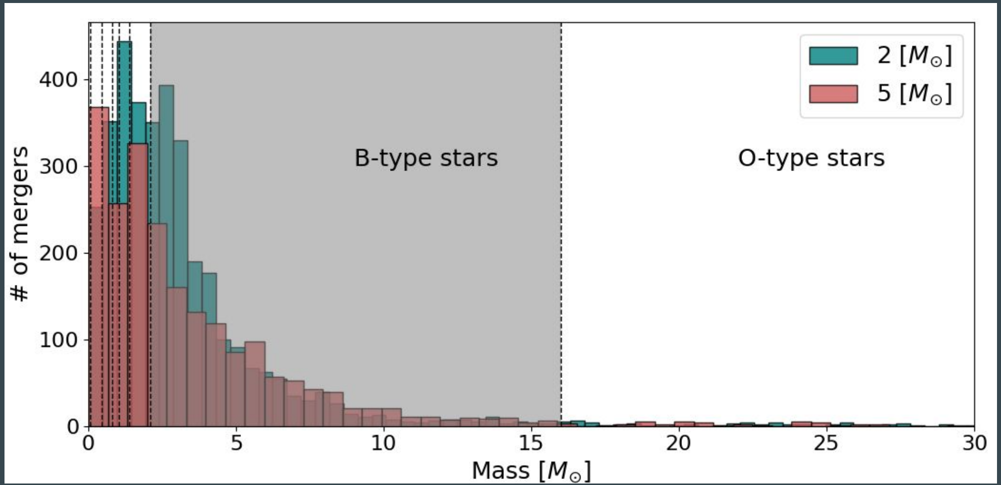

Possible **progenitors of magnetic Ap stars** among late B-type FS CMa stars

Current view of FS CMa stars

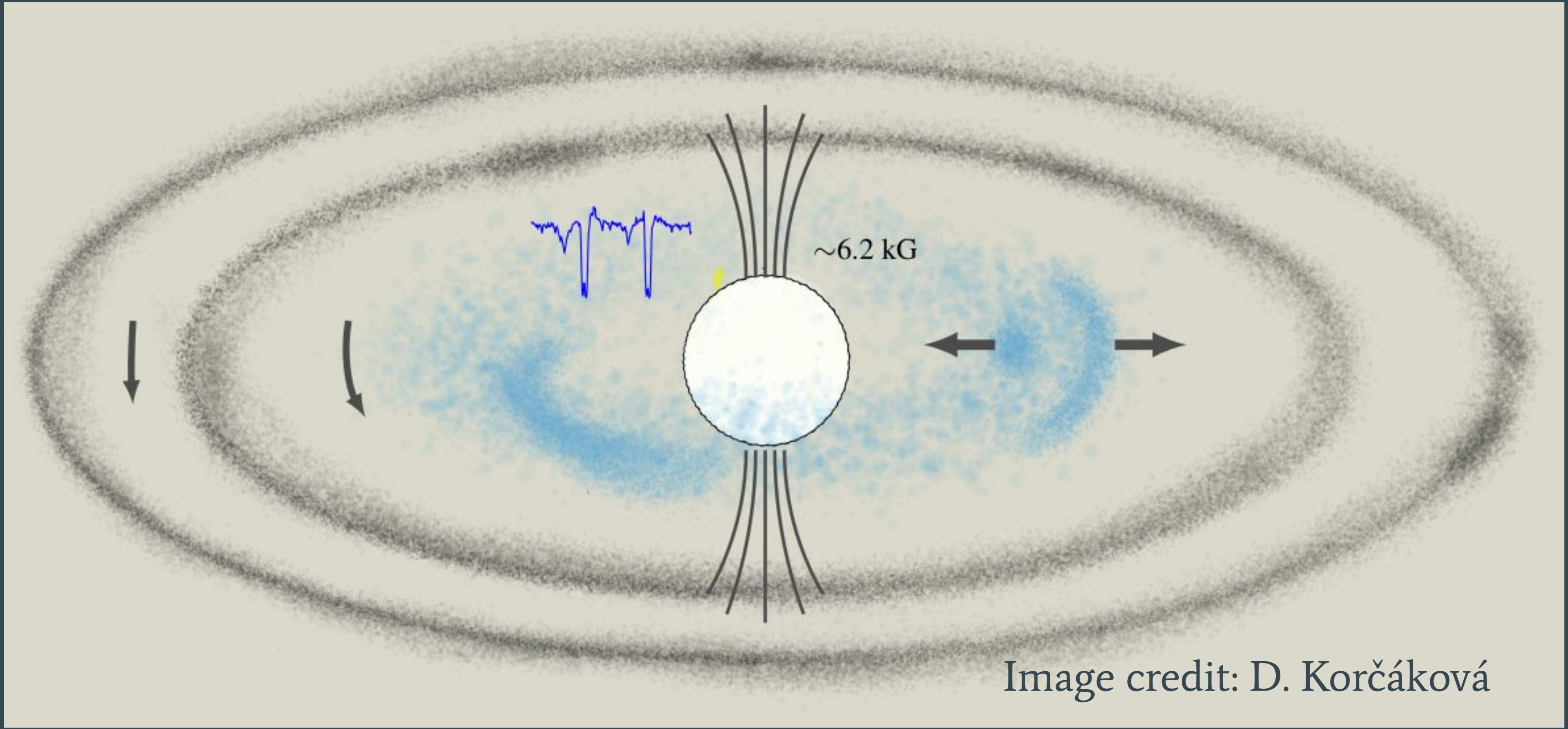

Evolutionary stages of the merger products

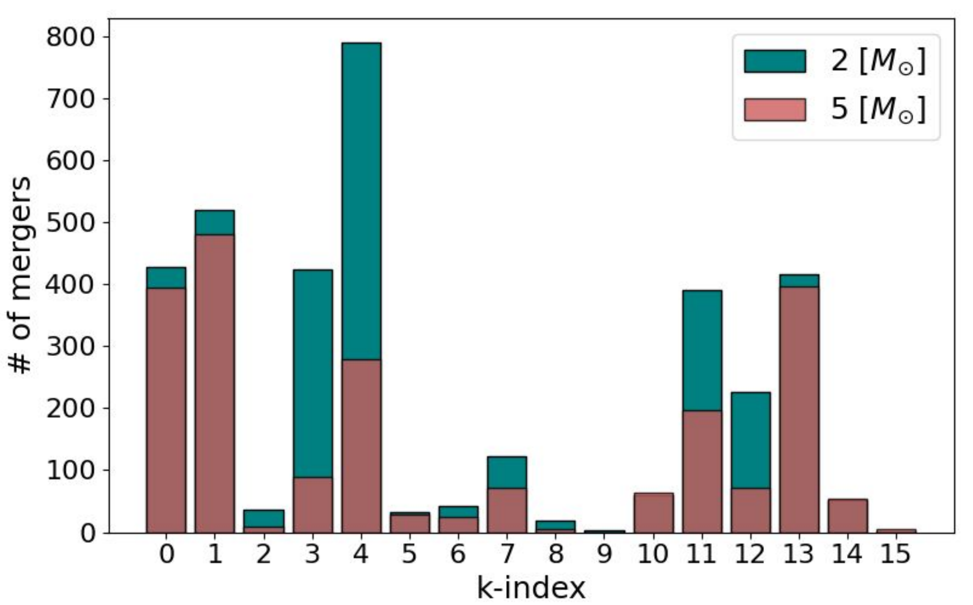

Dvořáková et al. (submitted)

Hurley et al. (2000)

0	MS fully convective
1	MS
2	Hertzsprung Gap
3	First Giant Branch
4	Core Helium Burning
5	Early AGB
6	Thermally Pulsing AGB
7	Naked Helium Star MS
8	Naked Helium Star Hertzsprung Gap
9	Naked Helium Star Giant Branch
10	Helium White Dwarf
11	Carbon/Oxygen White Dwarf
12	Oxygen/Neon White Dwarf
13	Neutron Star
14	Black Hole
15	massless remnant

Additional figures and tables

Spectral type	Stars at 0 Myr [%]		Stars involved in mergers [%]		Merger products [%]		Merger ratio [%]	
m_{thr}	2 $M_\odot$	5 $M_\odot$	2 $M_\odot$	5 $M_\odot$	2 $M_\odot$	5 $M_\odot$	2 $M_\odot$	5 $M_\odot$
O	0.11	0.12	2.23	3.32	2.47	3.46	30.99	26.22
B	**3.37**	**3.53**	**50.11**	**48.15**	**54.44**	**50.48**	**23.24**	**12.54**
A	2.64	2.77	13.42	11.49	14.28	15.18	7.77	4.80
F	3.21	3.28	8.33	8.95	9.56	7.11	4.27	1.90
G	3.95	4.05	6.75	6.53	5.71	3.88	2.07	0.84
K	15.18	15.29	9.94	10.71	7.39	10.29	0.70	0.59
M	71.53	70.97	9.22	10.82	6.10	8.81	0.12	0.11
BrDw	0	0	0	0.02	0.06	0.78	0	0

Dvořáková et al. (submitted)

Additional figures and tables

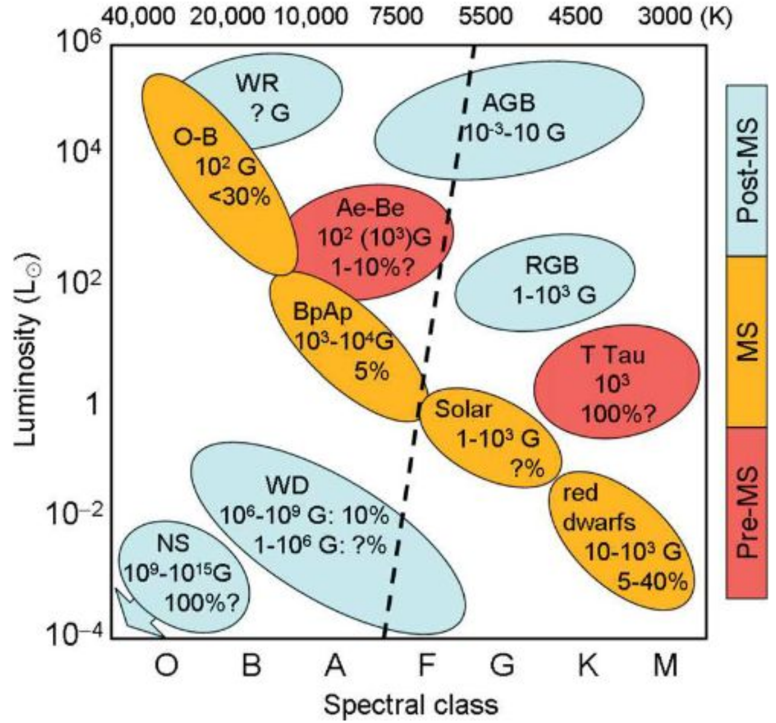

Figure 1. Occurence of magnetic fields across the H-R diagram in pre-MS, MS, and post-MS stars. Percentage indicates the fraction of stars of a given type to have such fields. The dashed line separates stars with convective (on the right) and radiative (on the left) envelops.

Berdyugina (2009)

Additional figures and tables

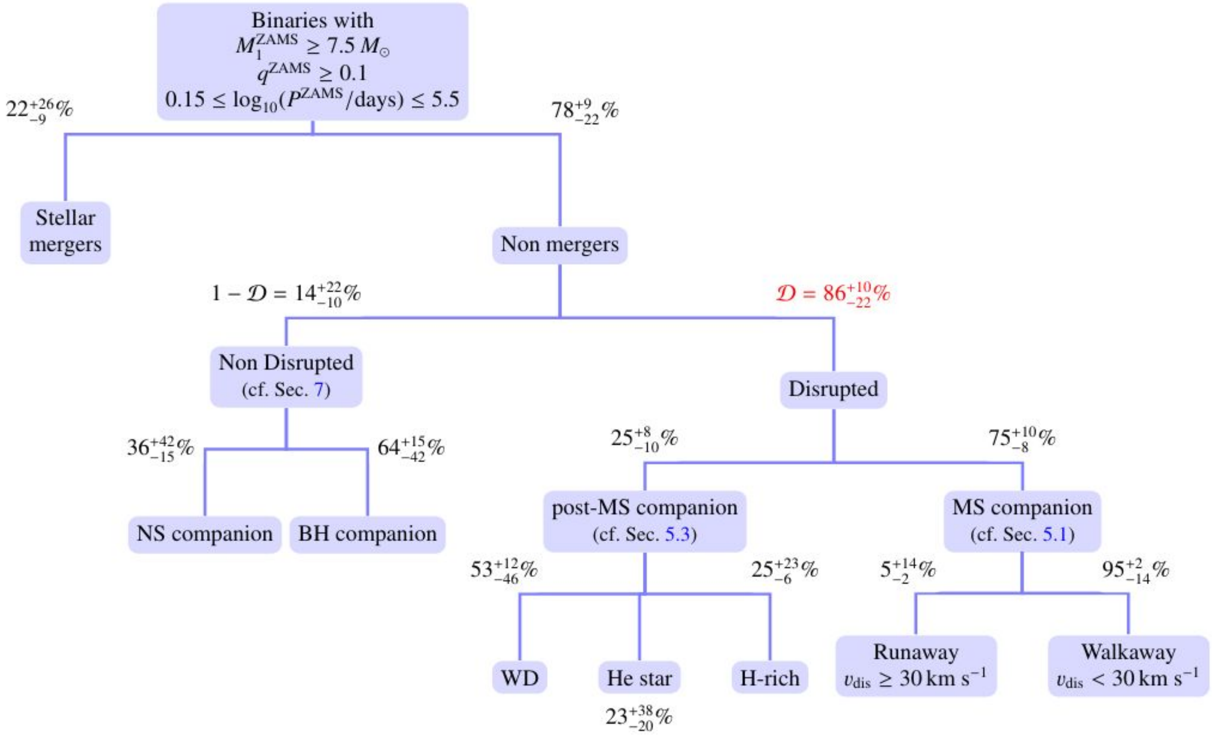

Fig. 4. Overview of the binary evolution scenarios up to the first CC event. The branching ratios shown are from our fiducial simulation, and we highlight in red the disruption fraction $\mathcal{D}$. The errors on each fraction exclude the run without SN kicks ($\sigma_{kick} = 0\,\mathrm{km\,s^{-1}}$), which produces an unrealistically low disruption fraction (cf. Table 1 and Sect. 6).

Renzo et al. (2019)